Novae and Super-Soft Sources in High-Resolution X-ray Spectroscopy

Jan-Uwe Ness
European Space Agency

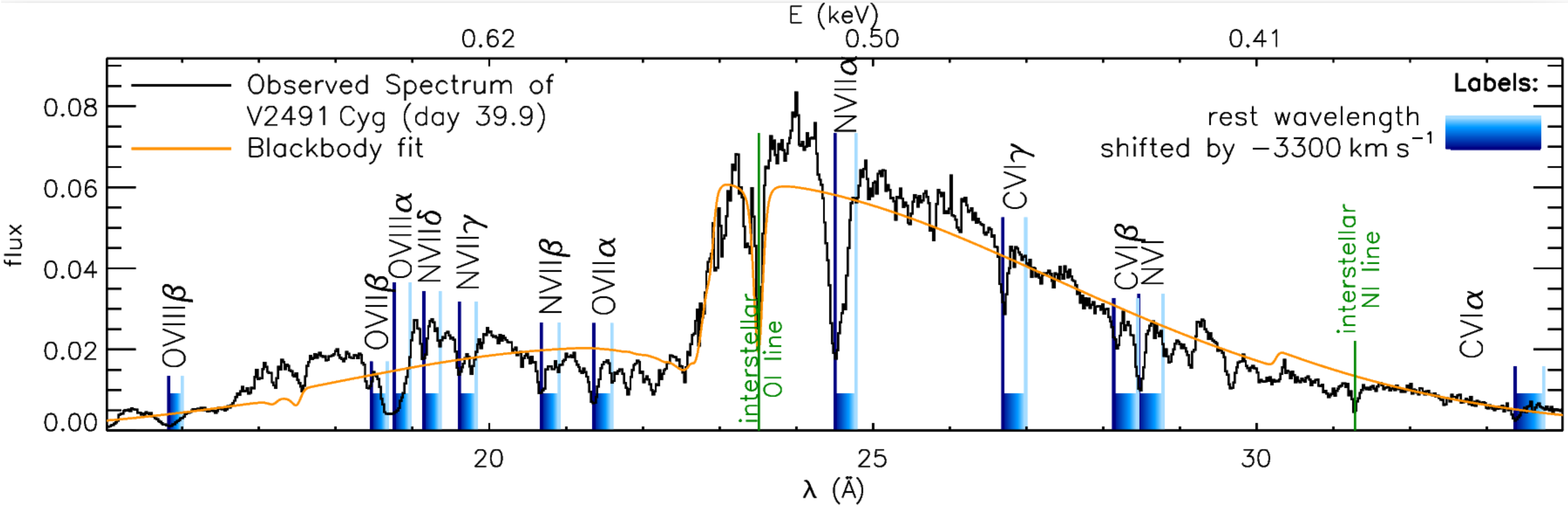

Nuclear burning in a low-gravity environment

Nuclear burning in a high-gravity environment

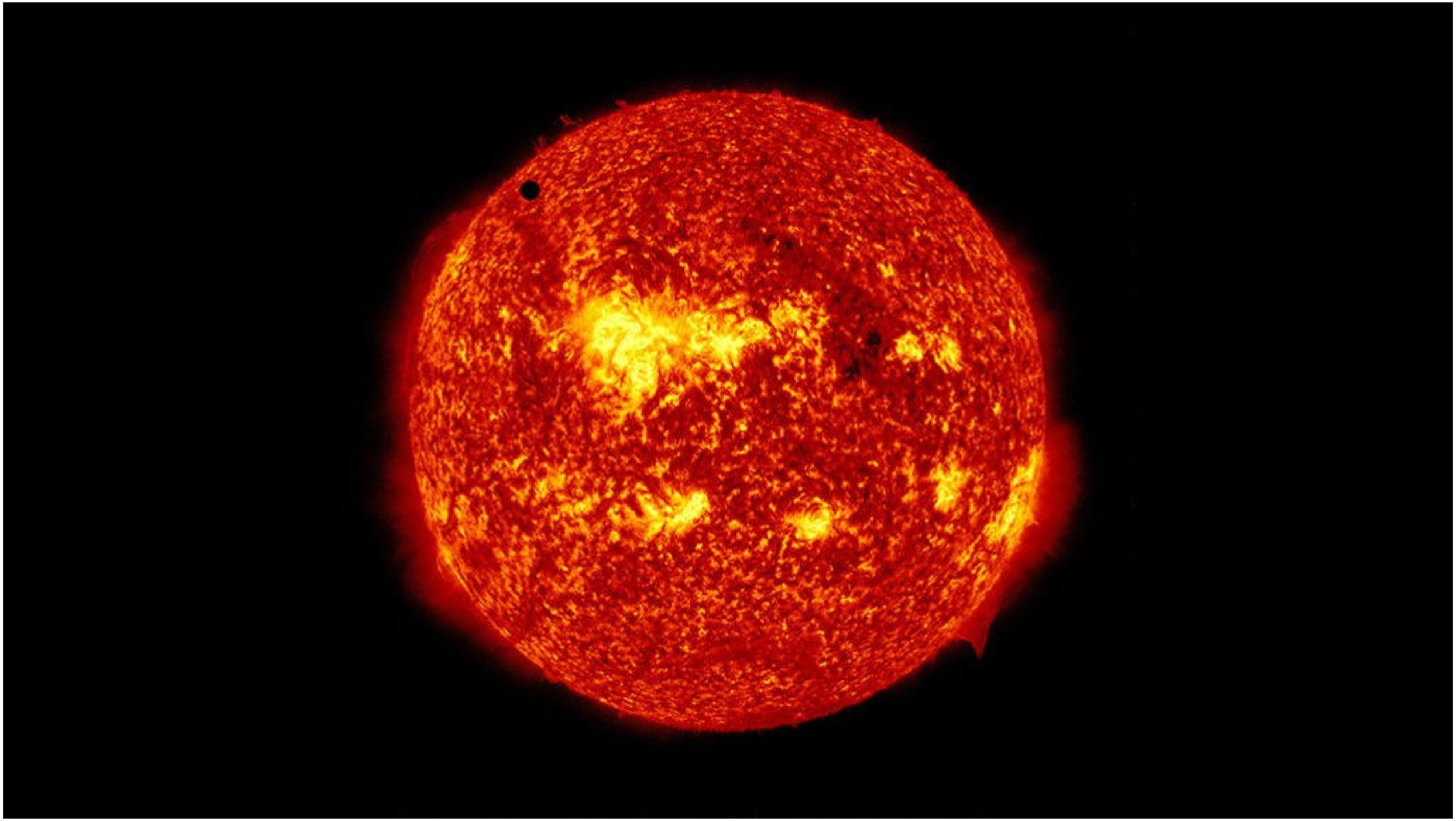

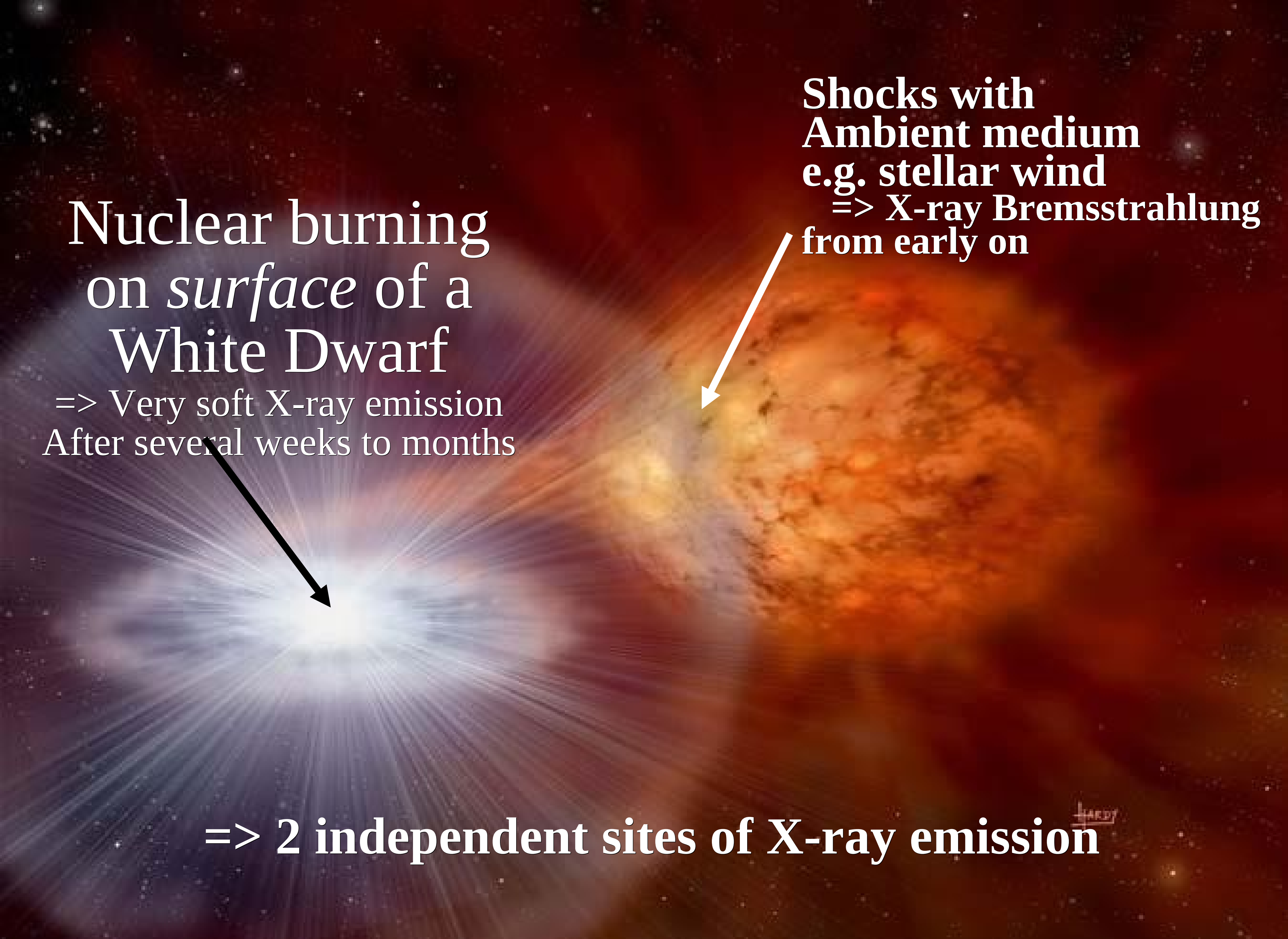
Shocks with
Ambient medium
e.g. stellar wind
=> X-ray Bremsstrahlung
from early on
Nuclear burning
on *surface* of a
White Dwarf
=> Very soft X-ray emission
After several weeks to months
=> 2 independent sites of X-ray emission

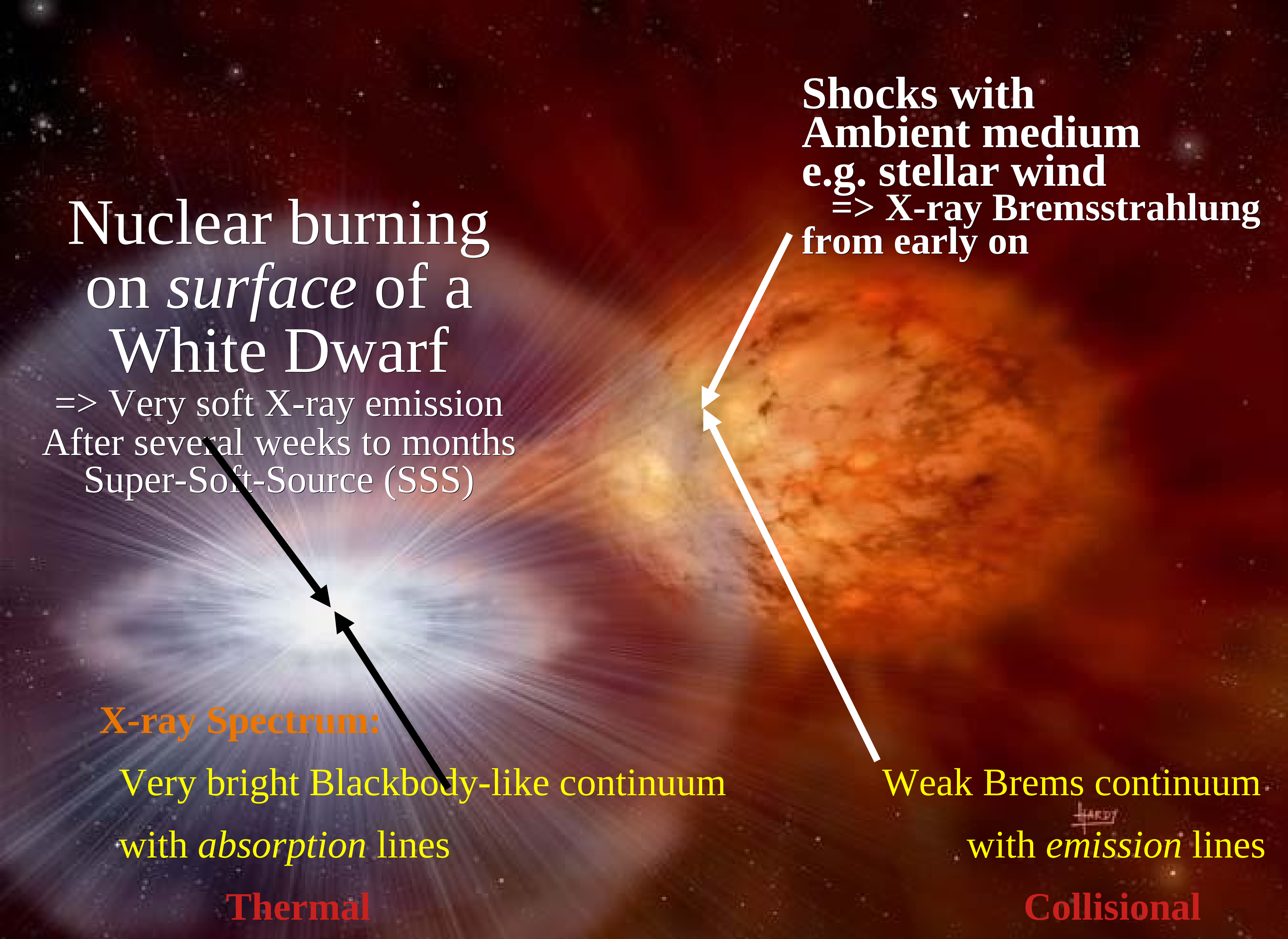

Nuclear burning on *surface* of a White Dwarf
=> Very soft X-ray emission
After several weeks to months
Super-Soft-Source (SSS)
Shocks with Ambient medium e.g. stellar wind
=> X-ray Bremsstrahlung from early on
X-ray Spectrum:
Very bright Blackbody-like continuum with *absorption* lines
Thermal
Weak Brems continuum with *emission* lines
Collisional

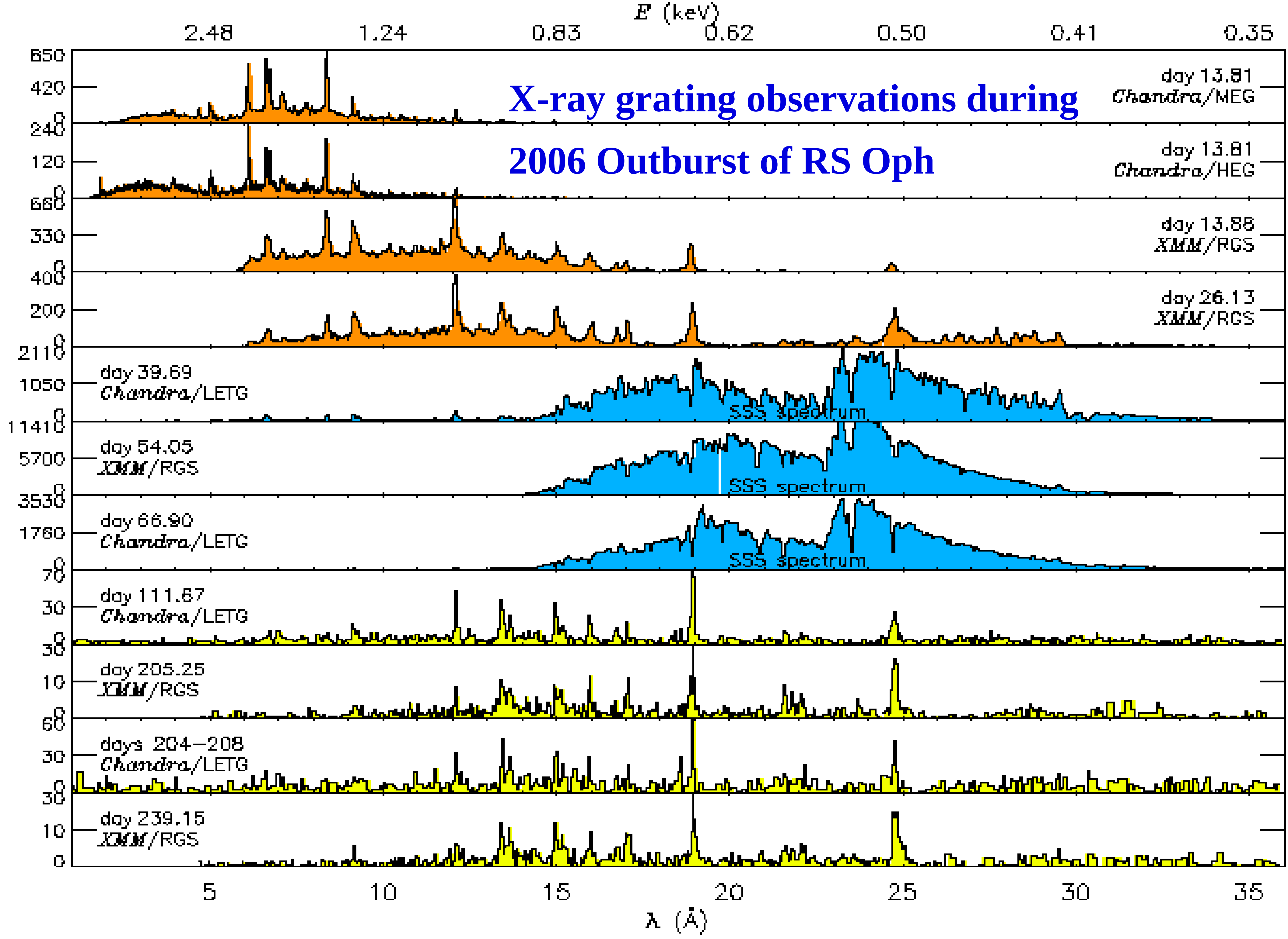
X-ray grating observations during
2006 Outburst of RS Oph
E (keV)
2.48
1.24
0.83
0.62
0.50
0.41
0.35
day 13.81
Chandra/MEG
day 13.81
Chandra/HEG
day 13.88
XMM/RGS
day 26.13
XMM/RGS
day 39.69
Chandra/LETG
SSS spectrum
day 54.05
XMM/RGS
SSS spectrum
day 66.90
Chandra/LETG
SSS spectrum
day 111.67
Chandra/LETG
day 205.25
XMM/RGS
days 204–208
Chandra/LETG
day 239.15
XMM/RGS
650
420
240
120
660
330
400
200
2110
1050
11410
5700
3530
1760
70
30
30
10
60
30
30
10
0
5
10
15
20
25
30
35
λ (Å)

Spectral evolution of Novae

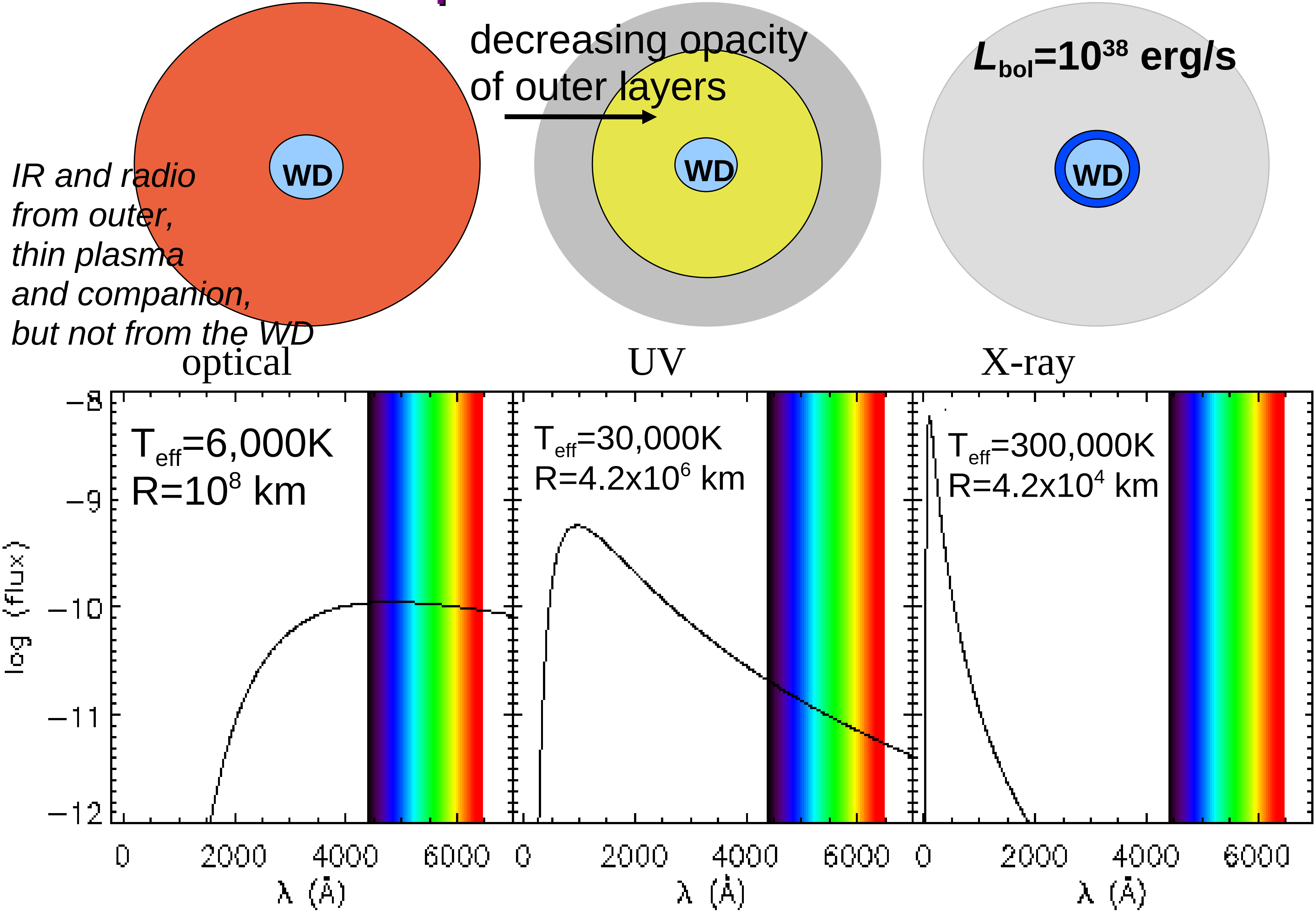

Spectral evolution of Novae

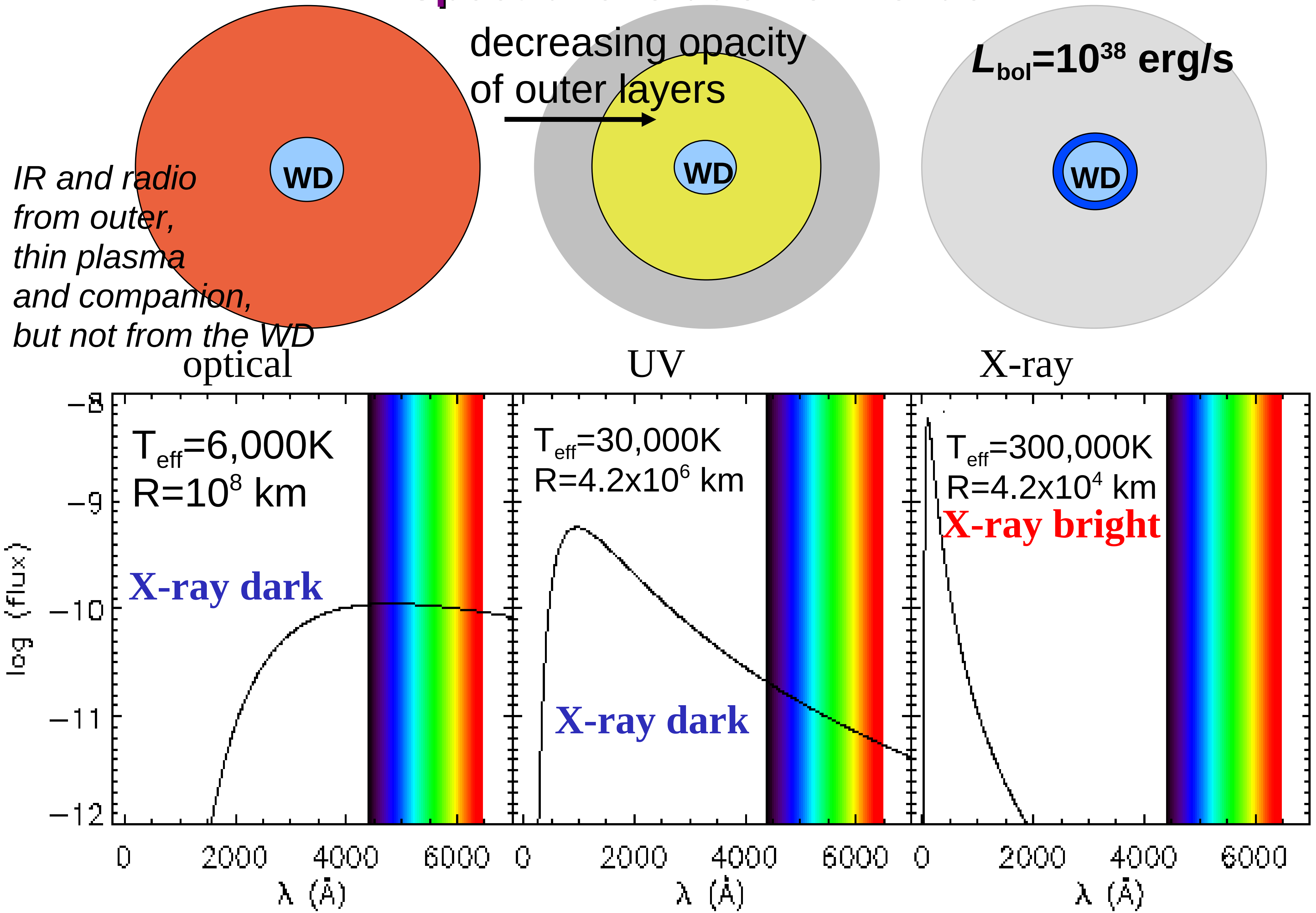

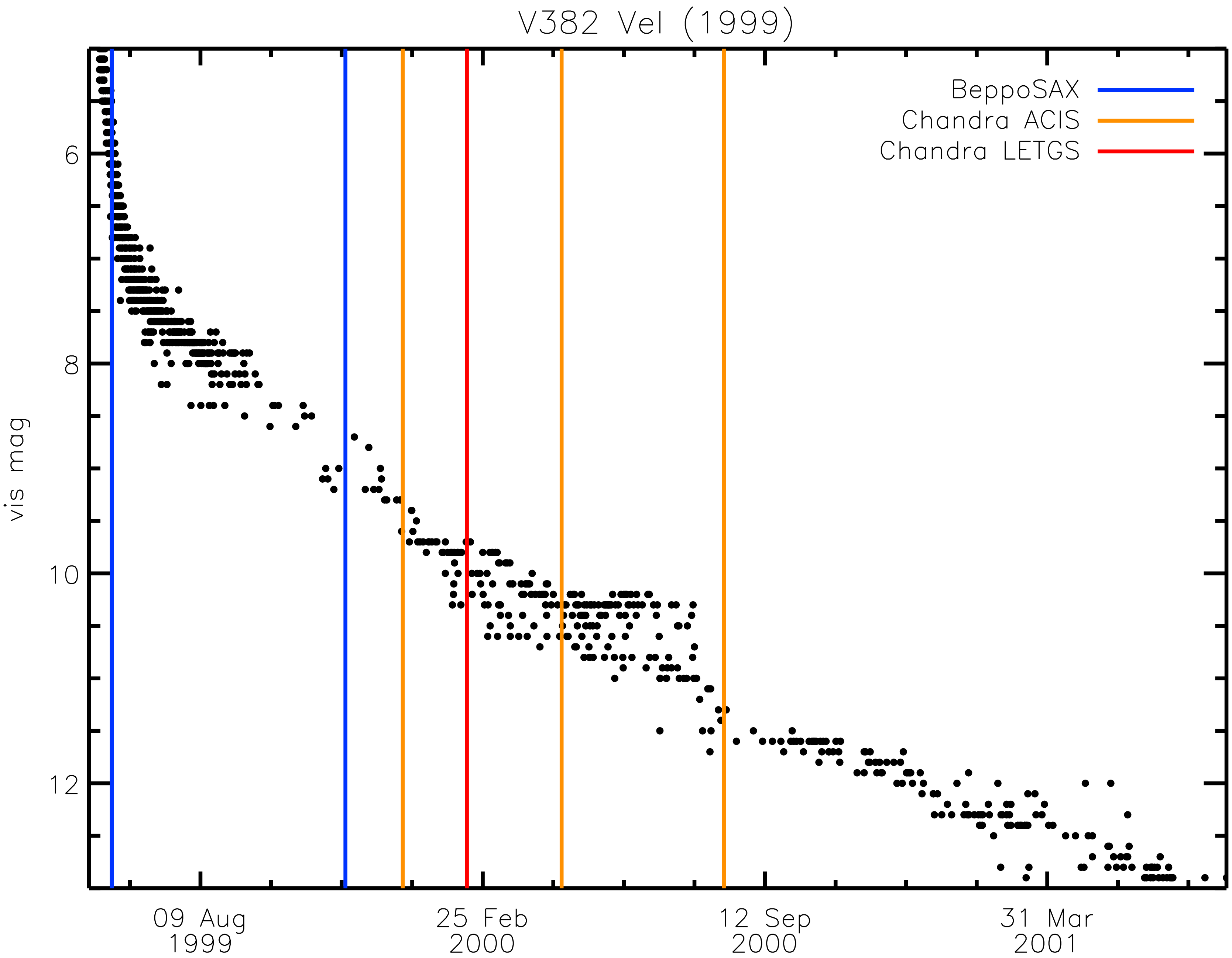
V382 Vel (1999)
BeppoSAX
Chandra ACIS
Chandra LETGS
vis mag
6
8
10
12
09 Aug 1999
25 Feb 2000
12 Sep 2000
31 Mar 2001

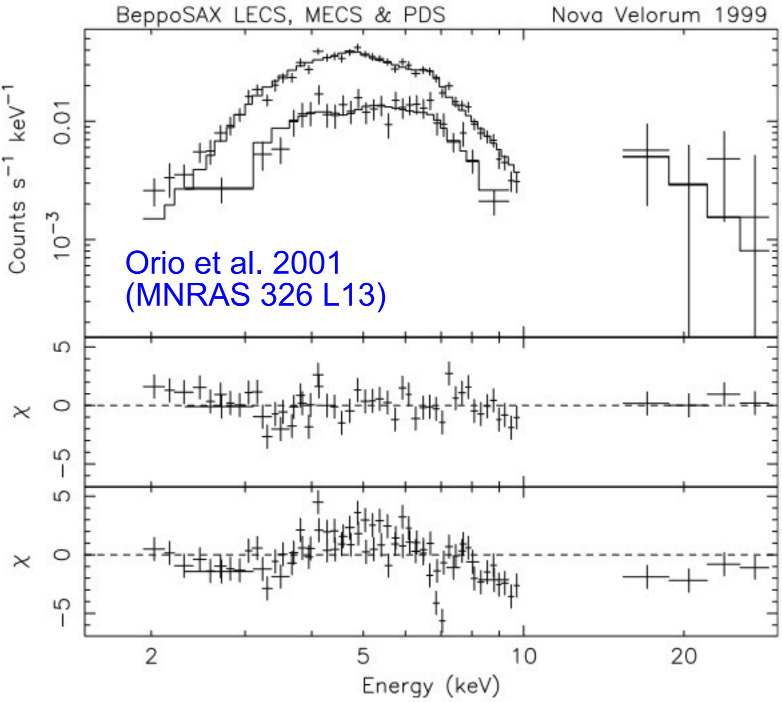

Figure 1. Observation of 1999 June: the LECS, MECS and PDS spectra and the best fit obtained with a VMEKAL model of a thermal plasma with depleted iron abundance (see text), enhanced abundance of all other elements (four times the solar value), $kT = 6.2$ keV, $N(\mathrm{H}) = 1.67 \times 10^{23}$ cm^{-2} (the reduced χ^2 is 1.13 per 83 dof). The residuals in units of σ are shown in the middle panel; below we plot the residuals of a fit done assuming solar abundances.

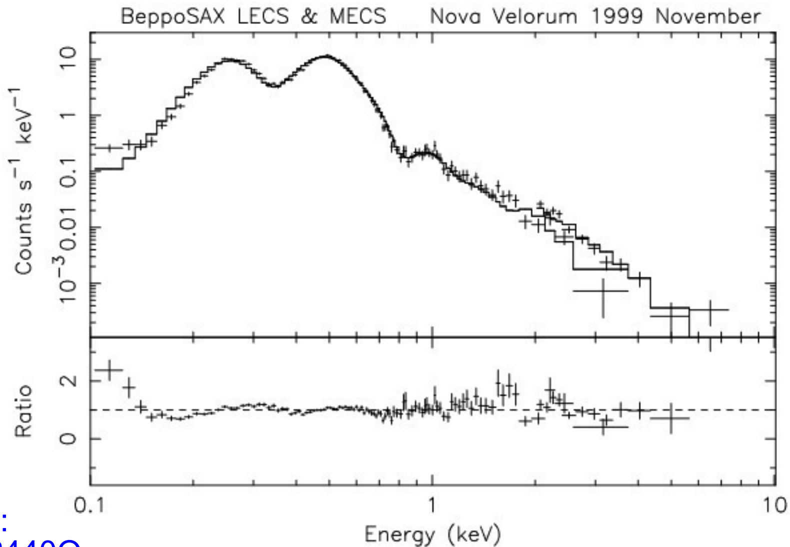

Orio et al. 2001:
2001astro.ph..2440O

Figure 1. Spectra observed in the 0.1-10 keV range with the BeppoSAX LECS and MECS in November 1999 and best fit with a model atmosphere studied by Hartmann & Heise (1997). The fit is not acceptable in the supersoft range where most of the flux is detected. The lower panel shows the residuals in counts per energy bin.

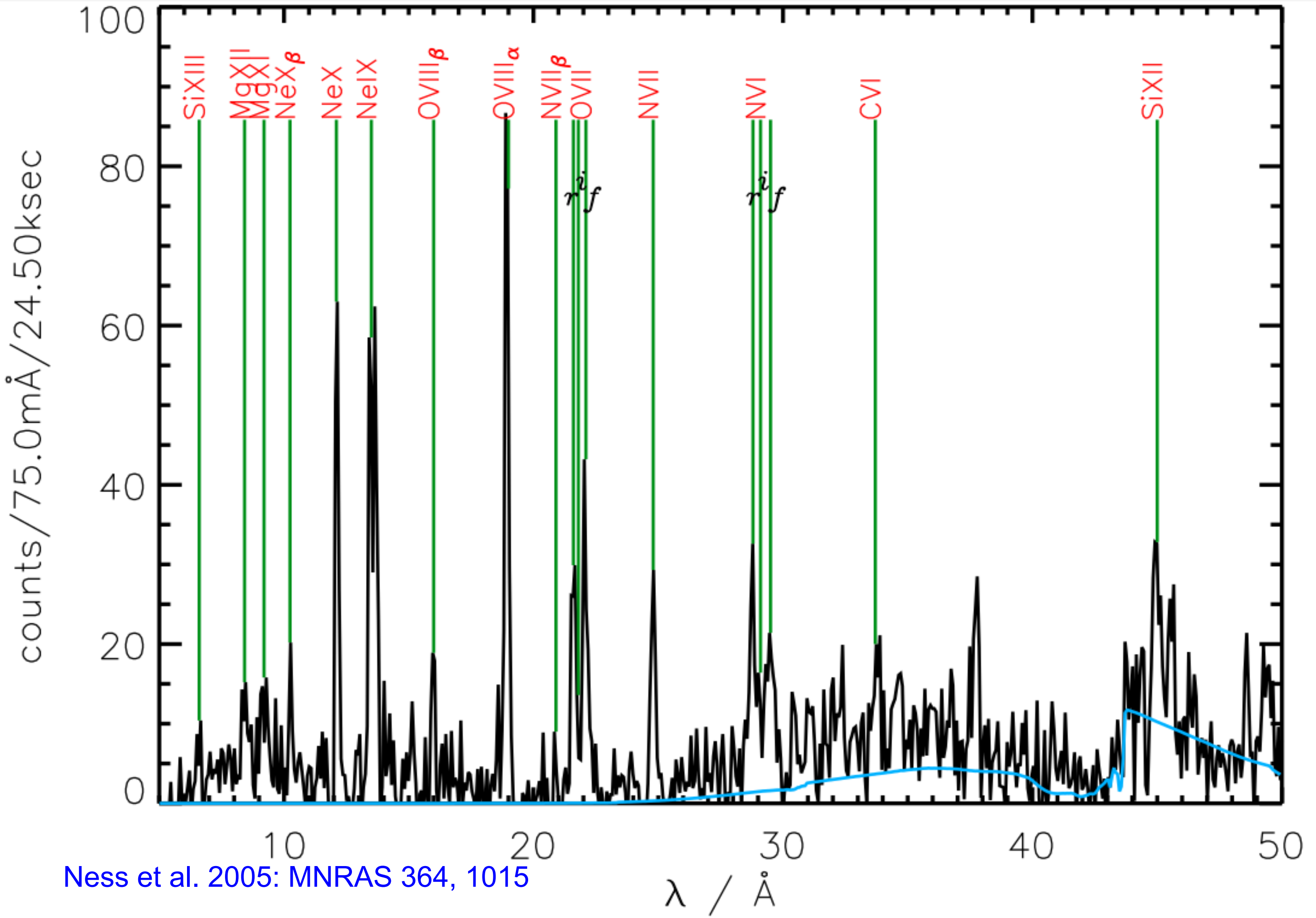

Ness et al. 2005: MNRAS 364, 1015

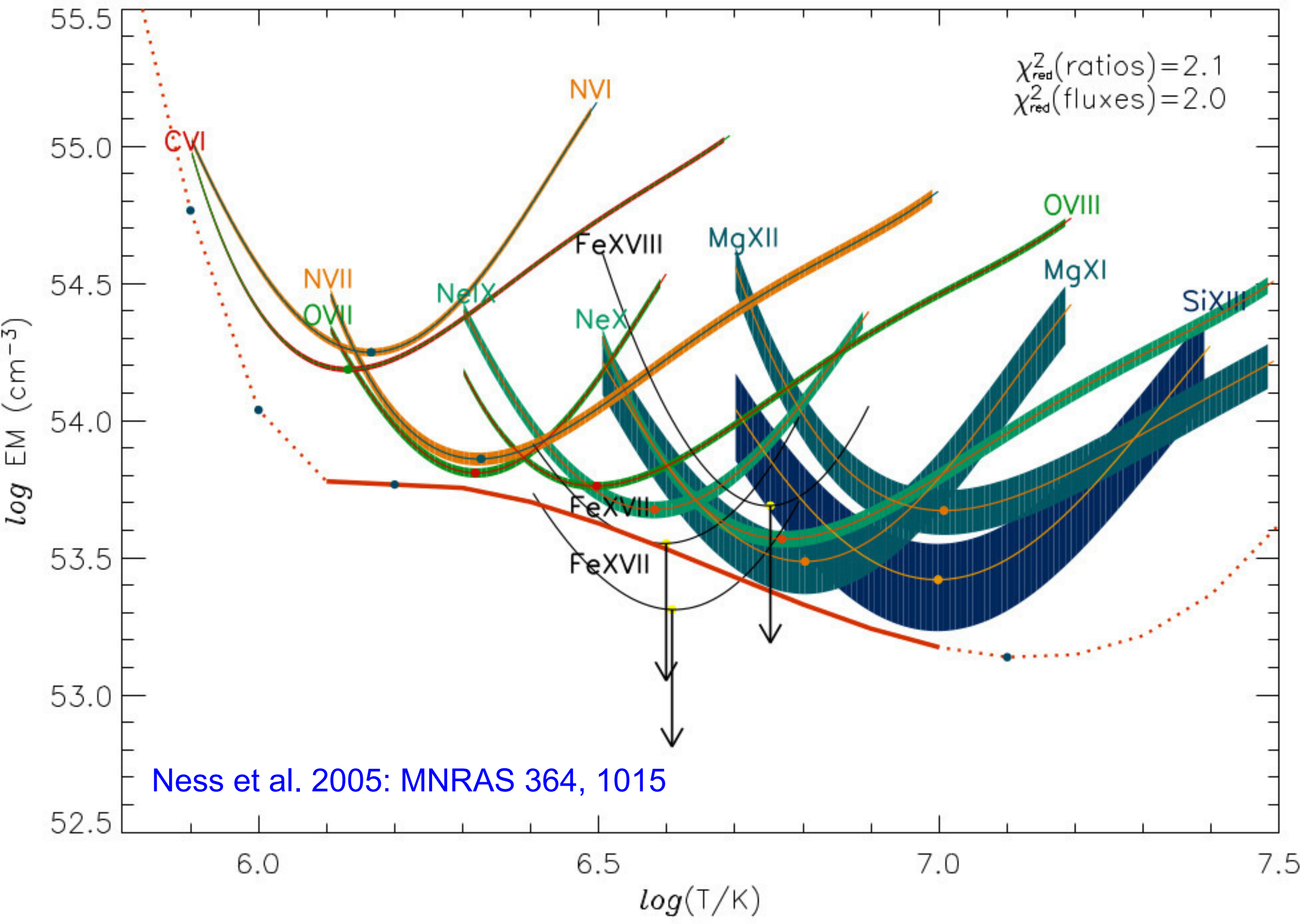

55.5
55.0
54.5
54.0
53.5
53.0
52.5
6.0
6.5
7.0
7.5
log EM (cm^{-3})
log(T/K)
χ^2_{red}(ratios)=2.1
χ^2_{red}(fluxes)=2.0
NVI
CVI
NVII
OVII
NeIX
NeX
FeXVIII
MgXII
OVIII
MgXI
SiXIII
FeXVII
FeXVII
Ness et al. 2005: MNRAS 364, 1015

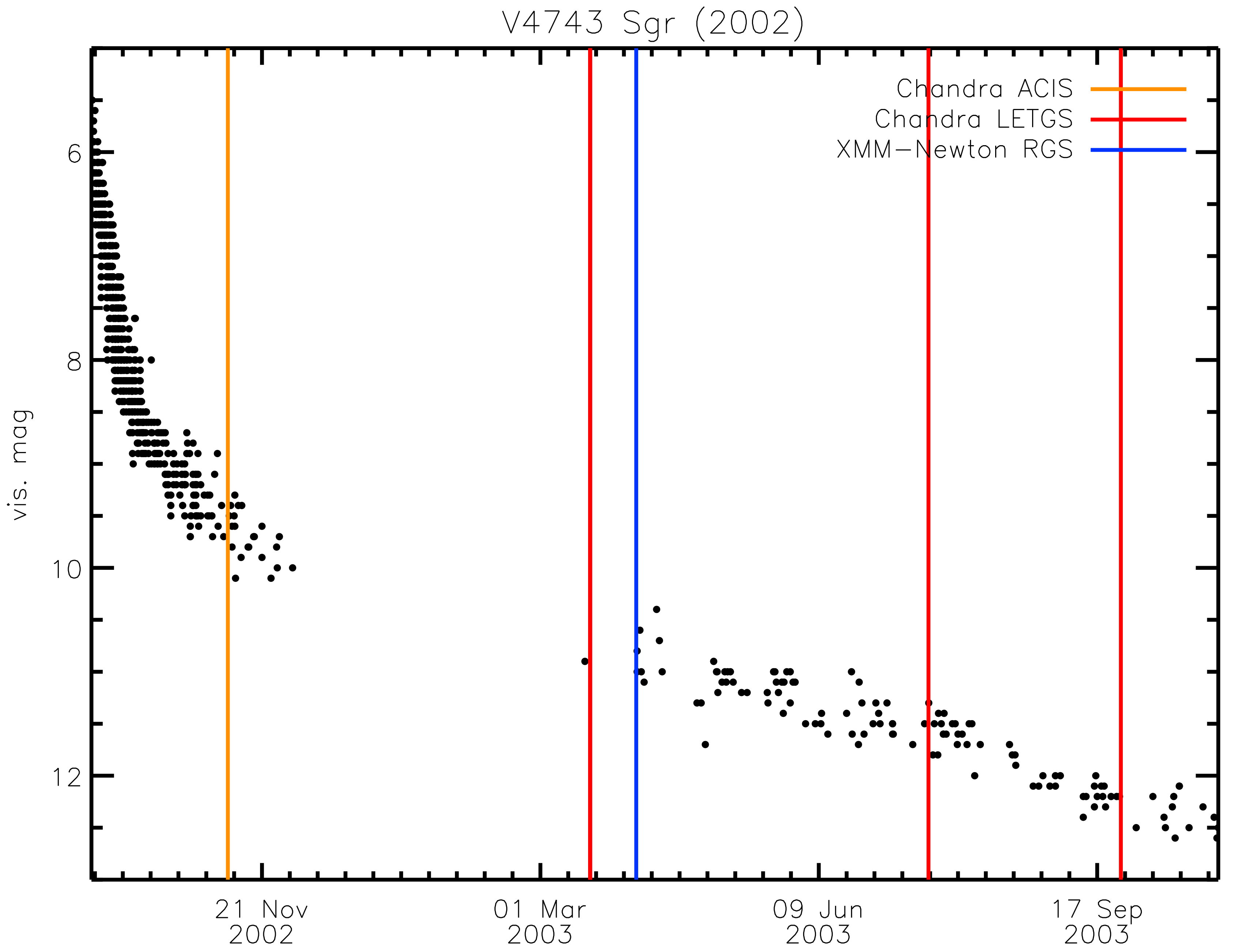
V4743 Sgr (2002)
Chandra ACIS
Chandra LETGS
XMM−Newton RGS
vis. mag
6
8
10
12
21 Nov 2002
01 Mar 2003
09 Jun 2003
17 Sep 2003

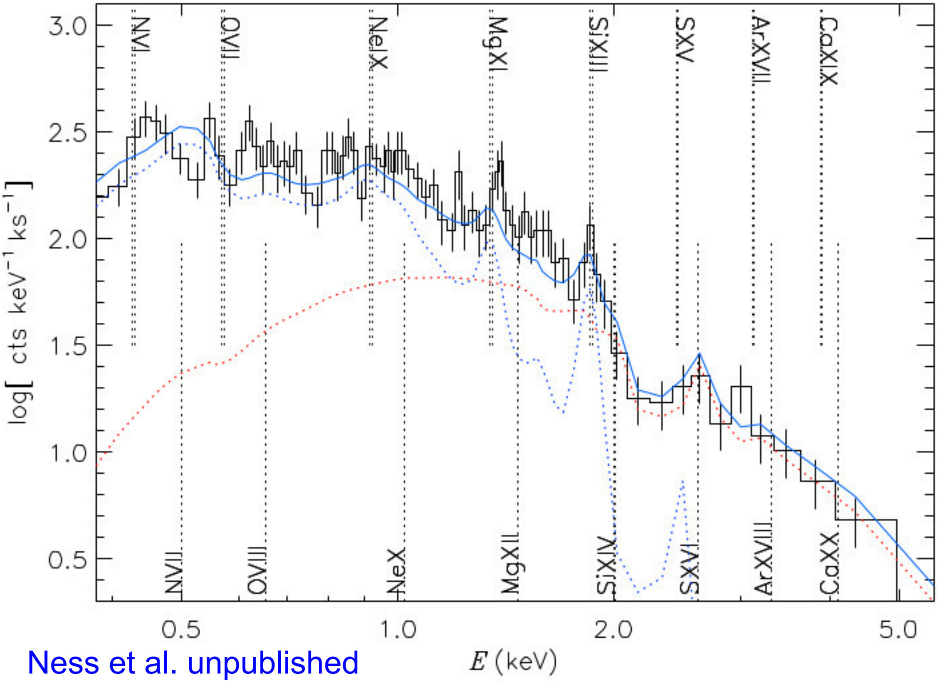

Ness et al. unpublished

Fig. 3. The ACIS-S spectrum obtained on day 50.2, before the SSS phase started. He-like and H-like lines are given in the top and bottom, respectively, and some emission features in the spectrum coincide with the expected wavelengths of emission lines of He-like ions (top labels) such as N VI, O VII, Mg XI, Si XIII, S XVI, and Ar XVII. Expected energies of H-like ions are indicated with labels in the bottom. The solid blue line is the best-fit 2-temperature VAPEC model, and the dotted blue and red lines indicate the respective low- and high-temperature components.

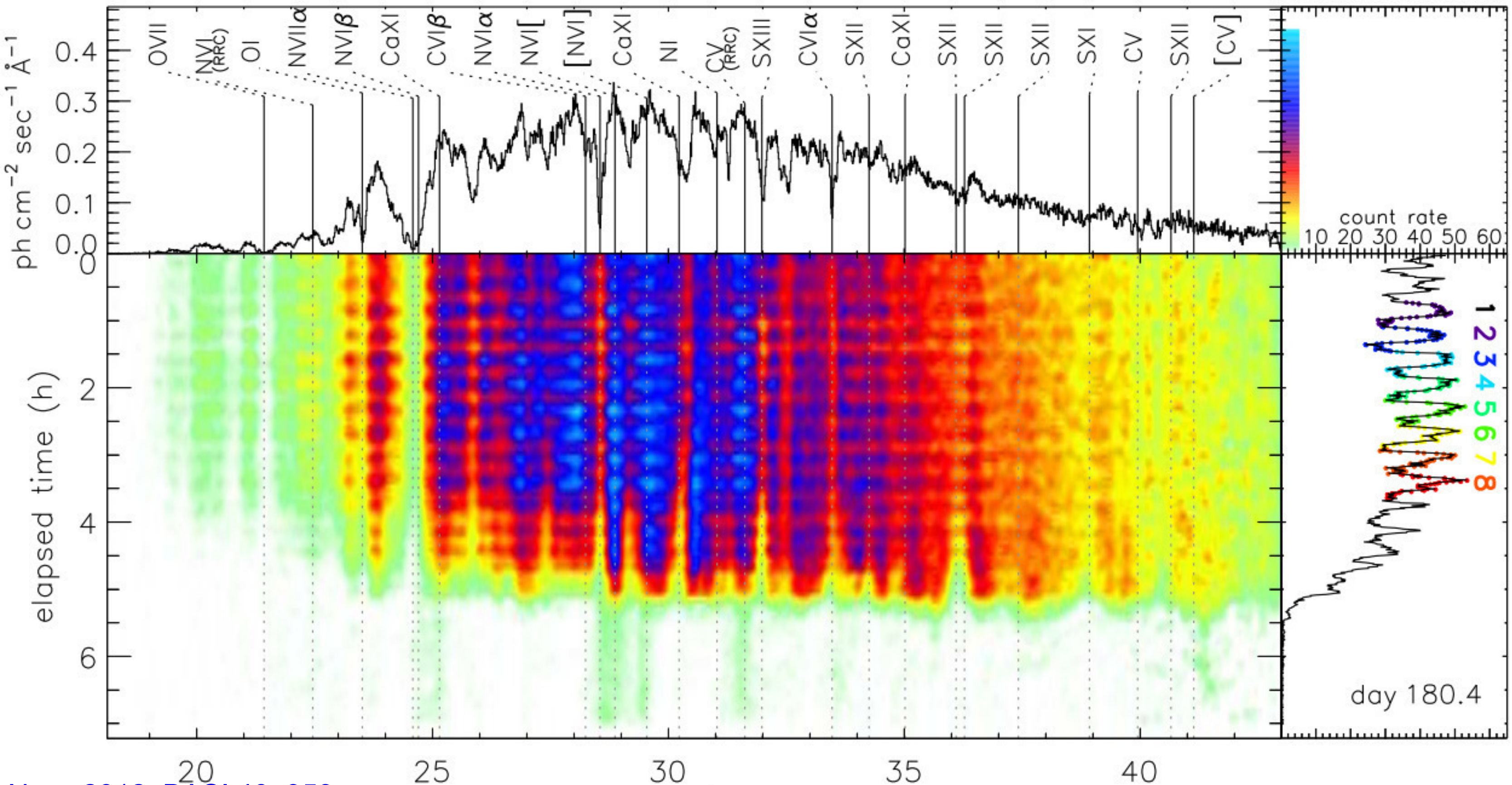

Ness 2012, BASI 40, 353

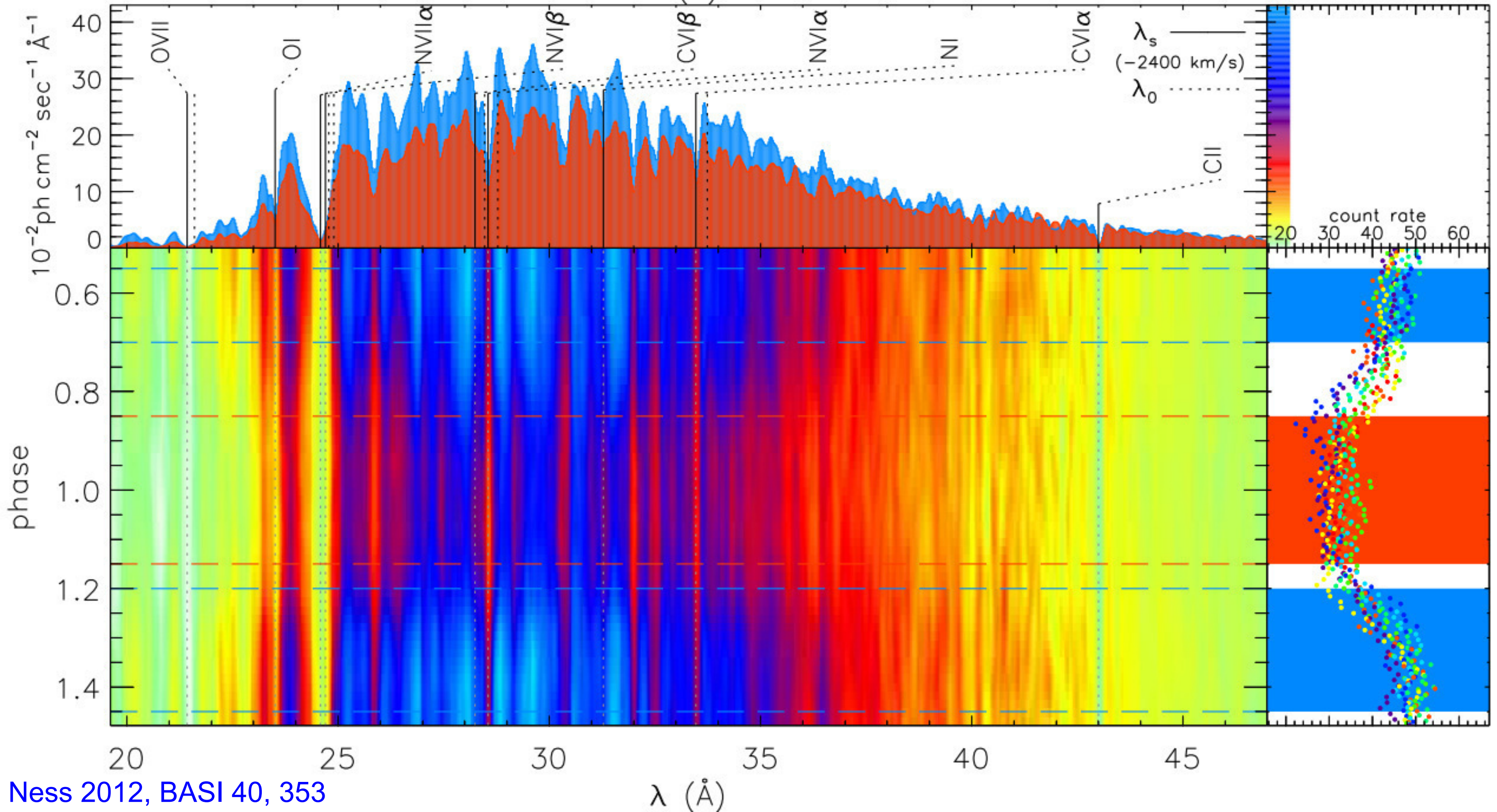

Ness 2012, BASI 40, 353

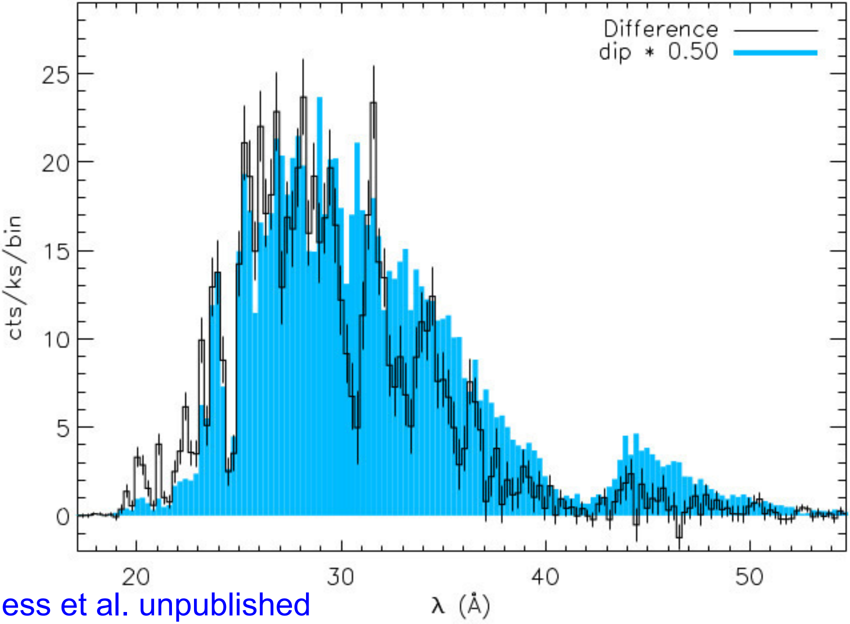

Ness et al. unpublished

Fig. 8. Difference spectrum illustrating changes during 1313-s oscillations. Shown are count spectra, thus not corrected for effective areas which are the same in both spectra. The light blue shading is the dip spectrum from Fig. 7, downscaled to match the peak of the difference spectrum. The difference spectrum has the characteristics of an atmosphere spectrum with more emission in the Wien tail and less emission in the soft tail whose shape is dominated by N_{H}. It may originate from deeper layers at higher temperature and stronger absorption.

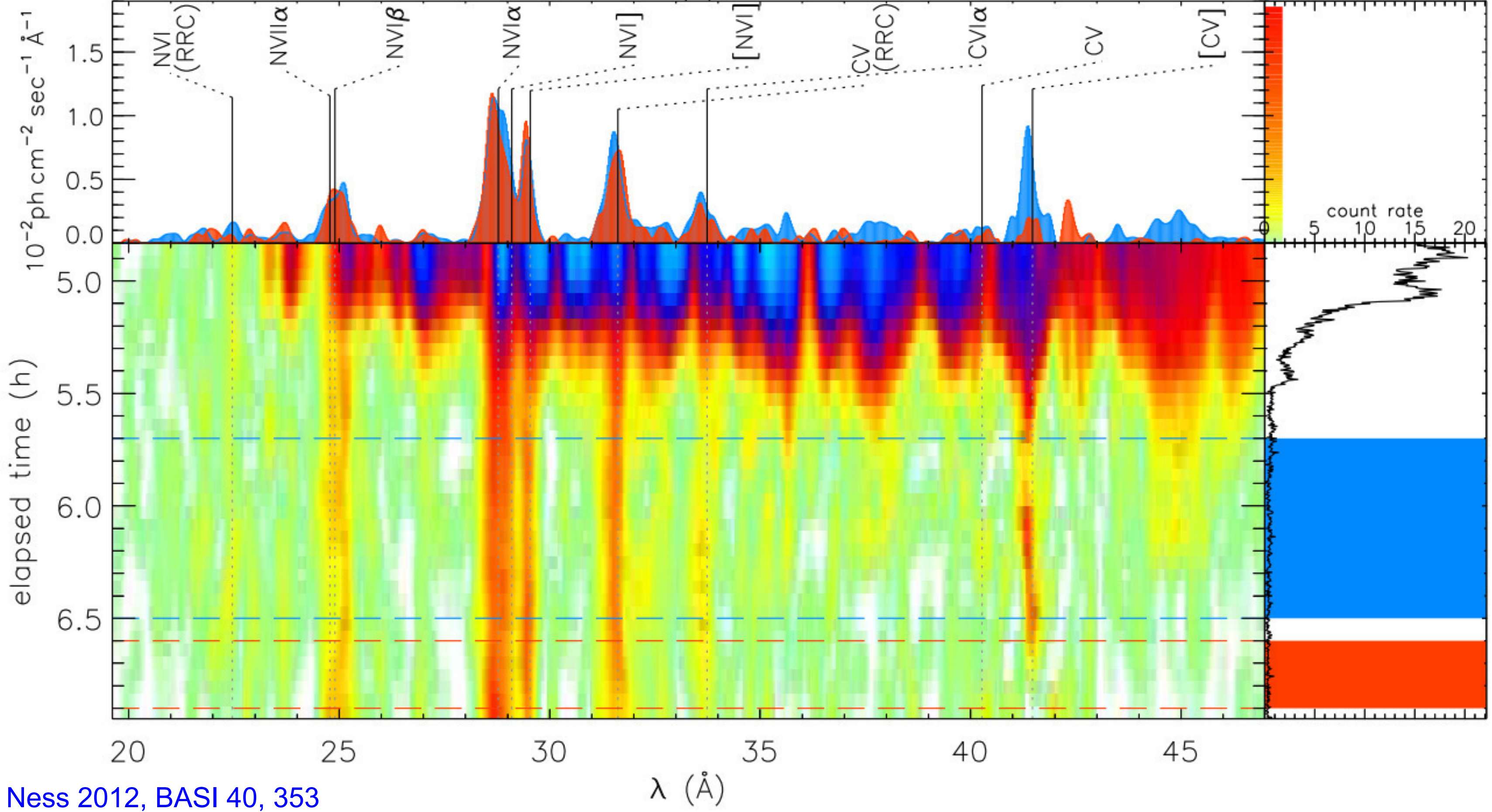

Ness 2012, BASI 40, 353

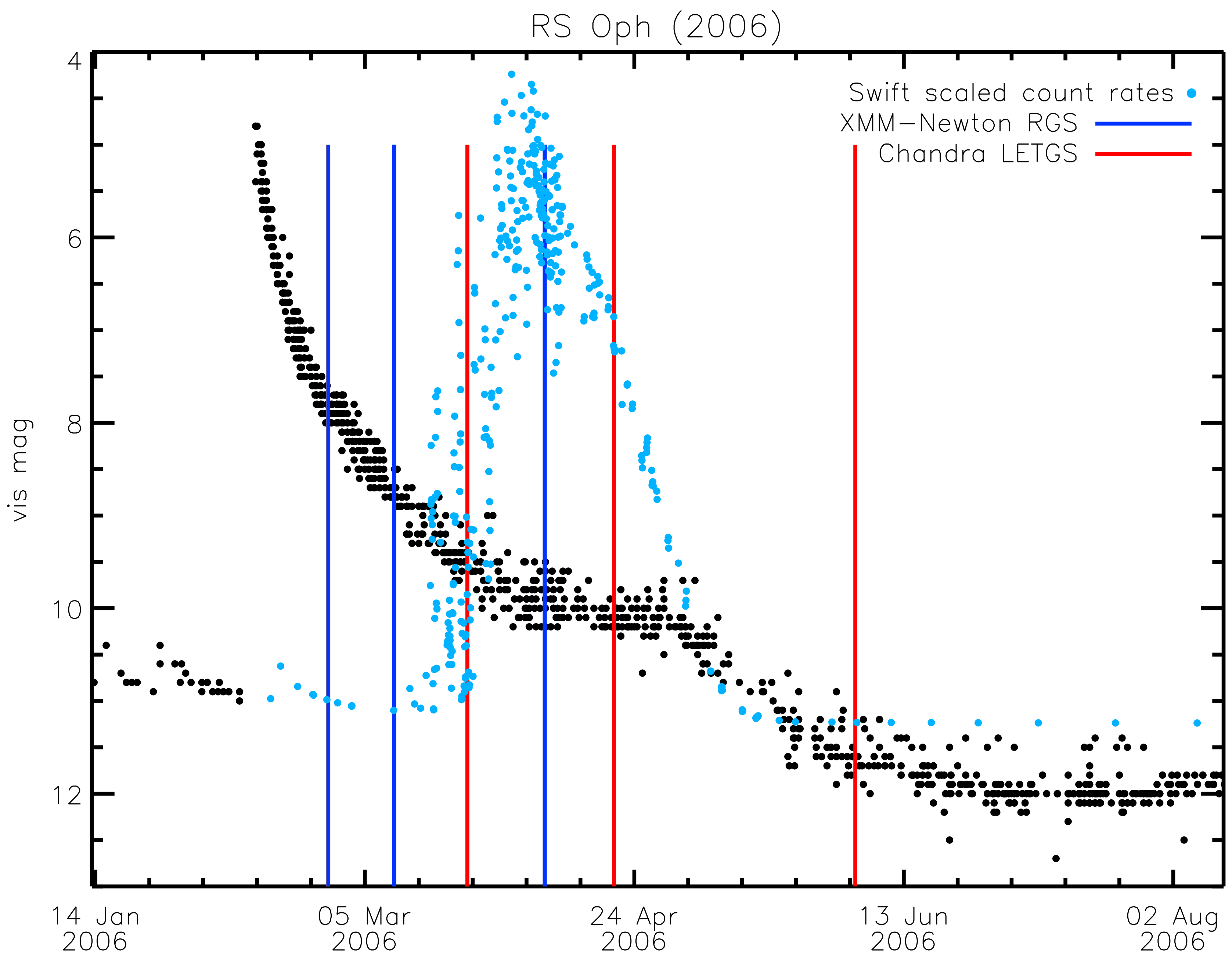

RS Oph (2006)
Swift scaled count rates
XMM−Newton RGS
Chandra LETGS
vis mag
4
6
8
10
12
14 Jan 2006
05 Mar 2006
24 Apr 2006
13 Jun 2006
02 Aug 2006

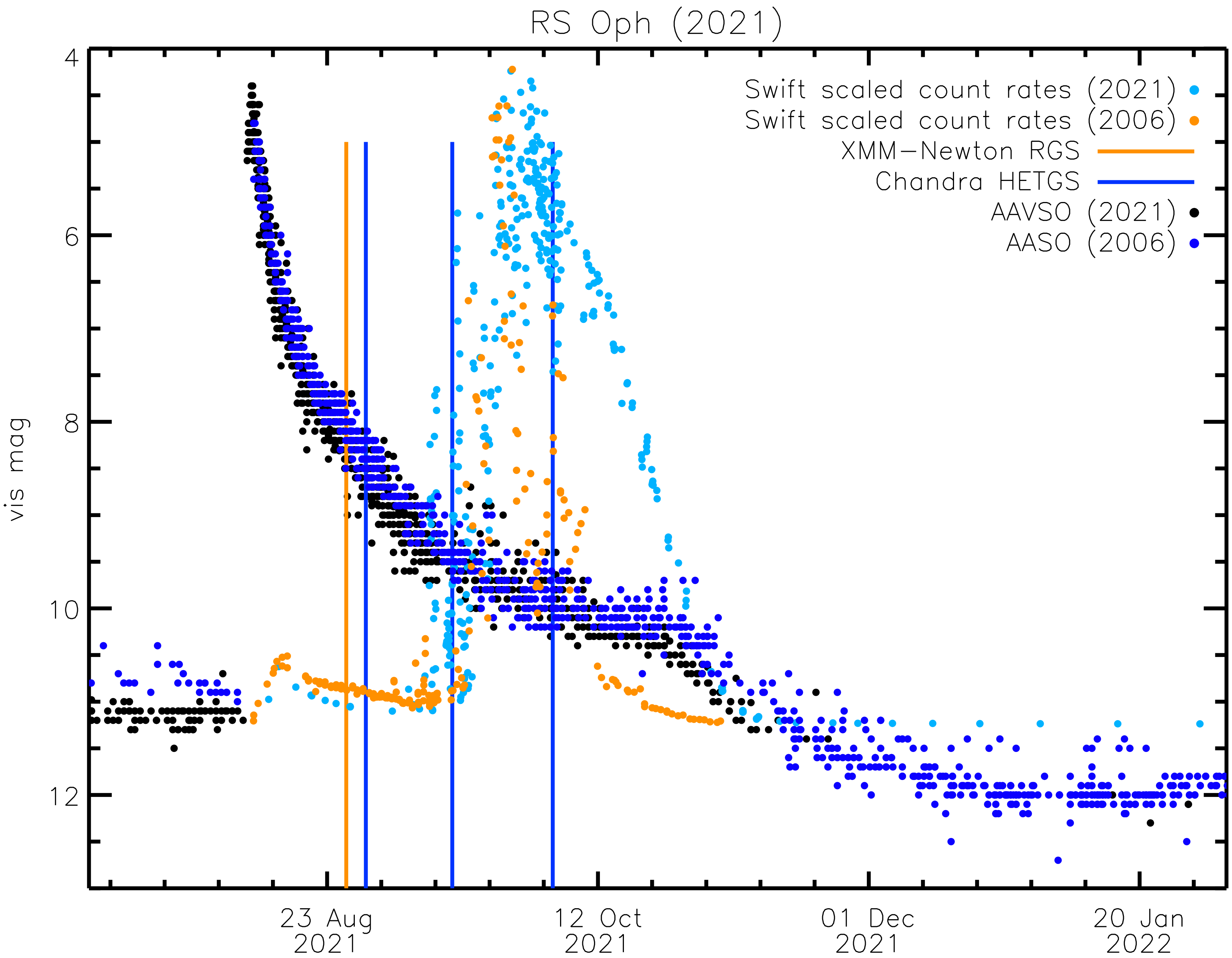
RS Oph (2021)
Swift scaled count rates (2021)
Swift scaled count rates (2006)
XMM−Newton RGS
Chandra HETGS
AAVSO (2021)
AASO (2006)
vis mag
4
6
8
10
12
23 Aug 2021
12 Oct 2021
01 Dec 2021
20 Jan 2022

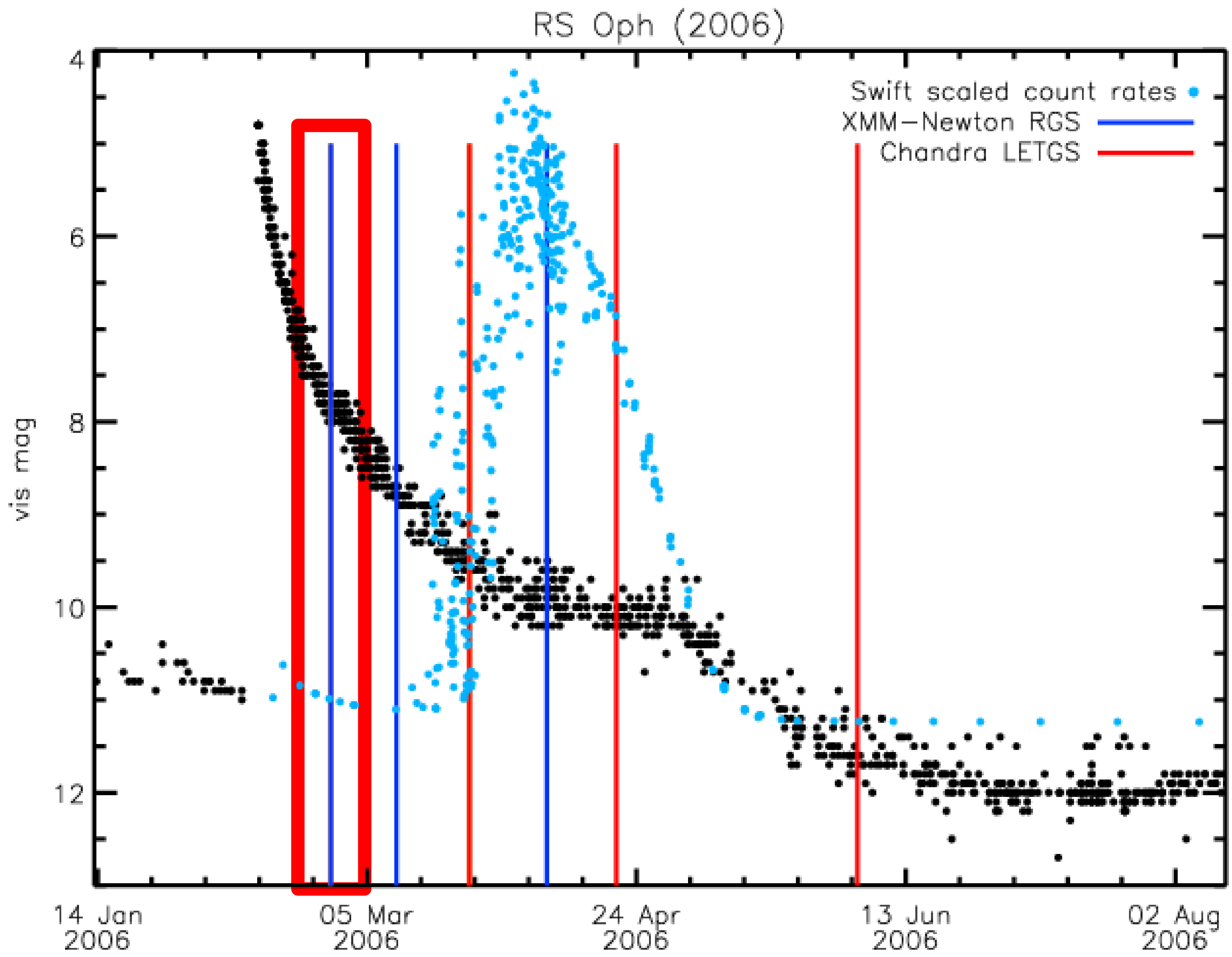

RS Oph (2006)
Swift scaled count rates
XMM−Newton RGS
Chandra LETGS
vis mag
4
6
8
10
12
14 Jan 2006
05 Mar 2006
24 Apr 2006
13 Jun 2006
02 Aug 2006

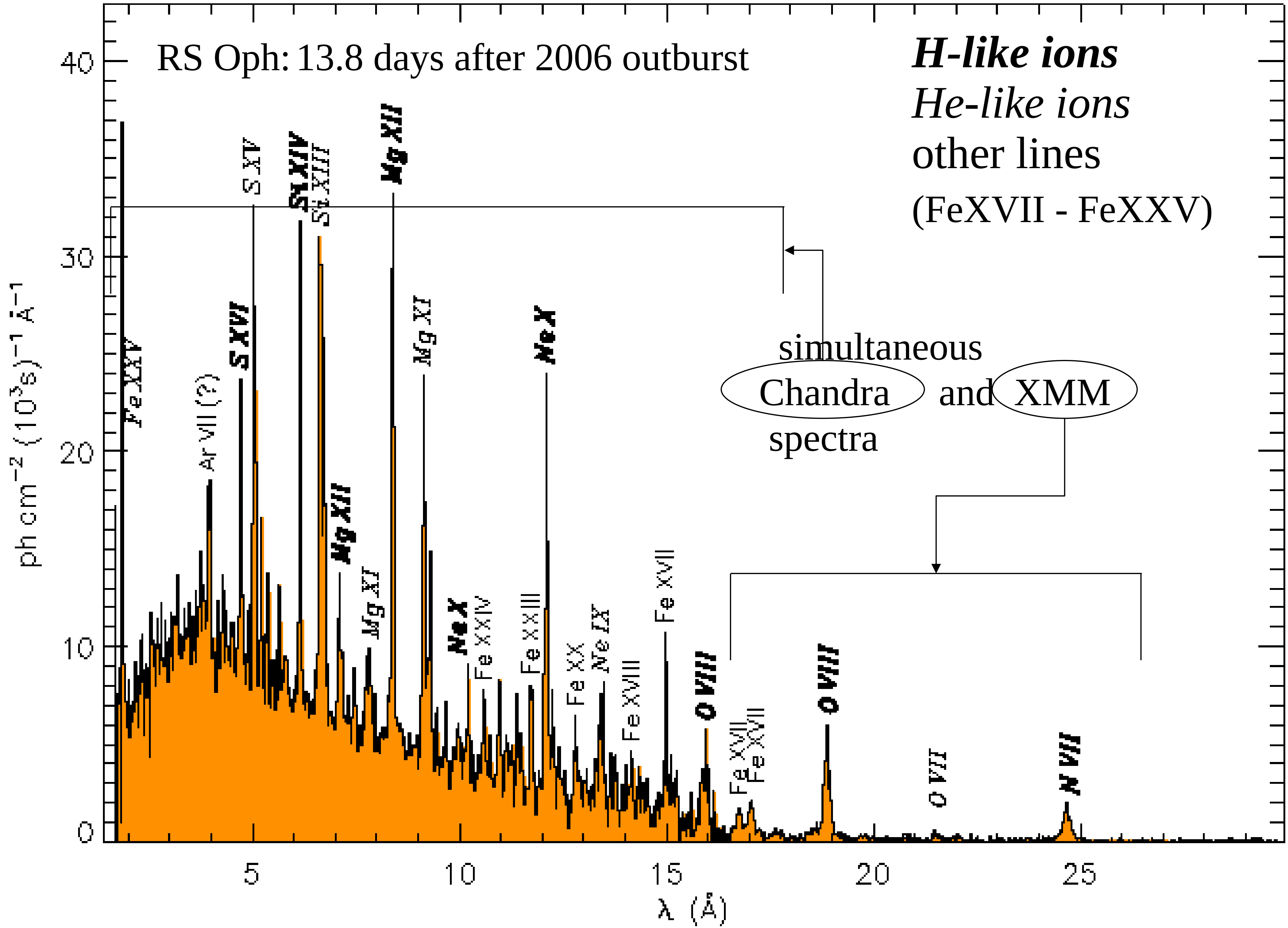

RS Oph: 13.8 days after 2006 outburst
H-like ions
He-like ions
other lines
(FeXVII - FeXXV)
simultaneous
Chandra
and
XMM
spectra
Fe XXV
Ar VII (?)
S XVI
S XV
Si XIV
Si XIII
Mg XII
Mg XI
Ne X
Fe XXIV
Fe XXIII
Fe XX
Ne IX
Fe XVIII
Fe XVII
O VIII
O VII
N VII
ph cm^{-2} (10^{3}s)$^{-1}$ Å^{-1}
λ (Å)

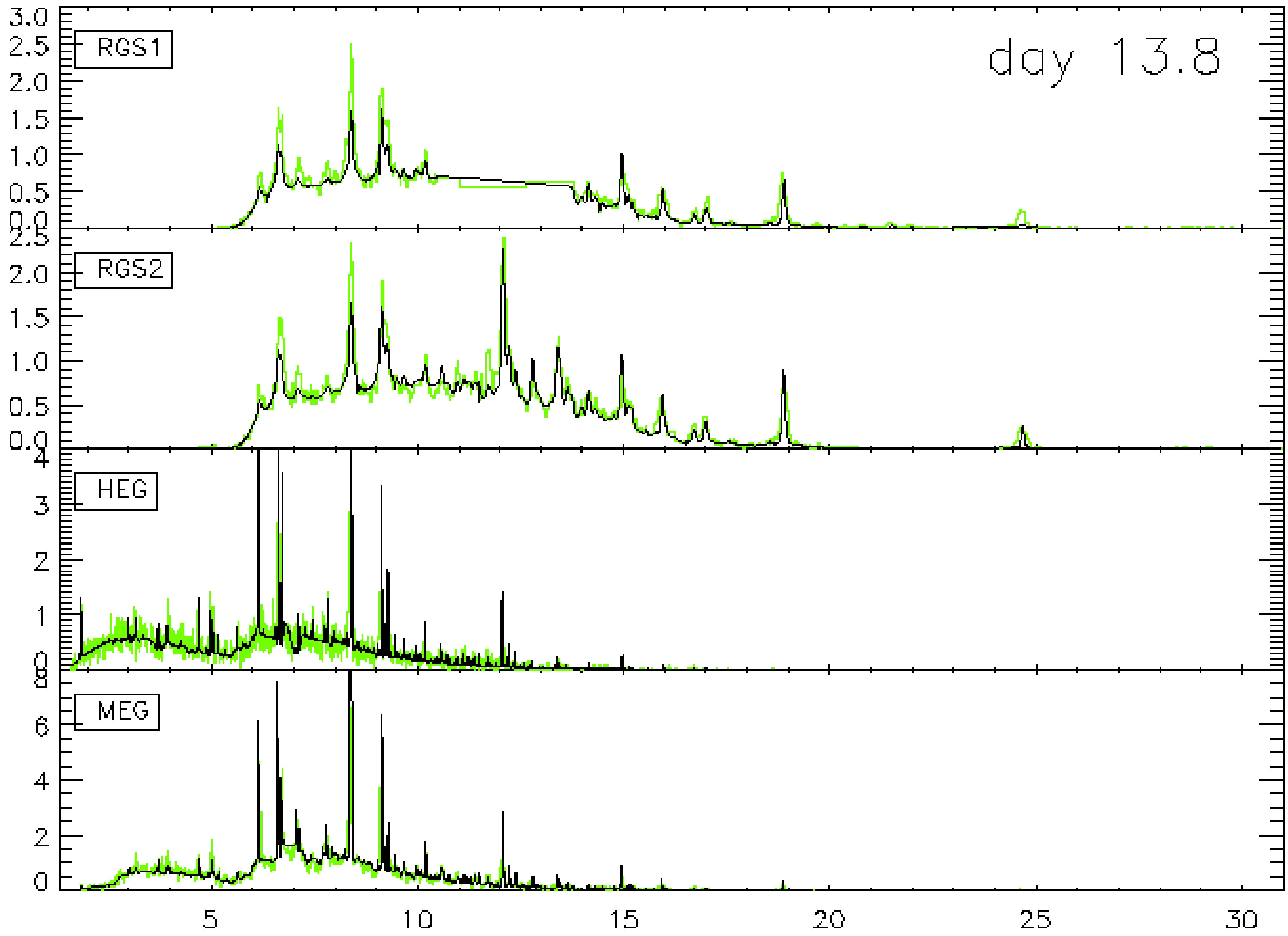

day 13.8
RGS1
RGS2
HEG
MEG
3.0
2.5
2.0
1.5
1.0
0.5
0.0
2.5
2.0
1.5
1.0
0.5
0.0
4
3
2
1
0
8
6
4
2
0
5
10
15
20
25
30

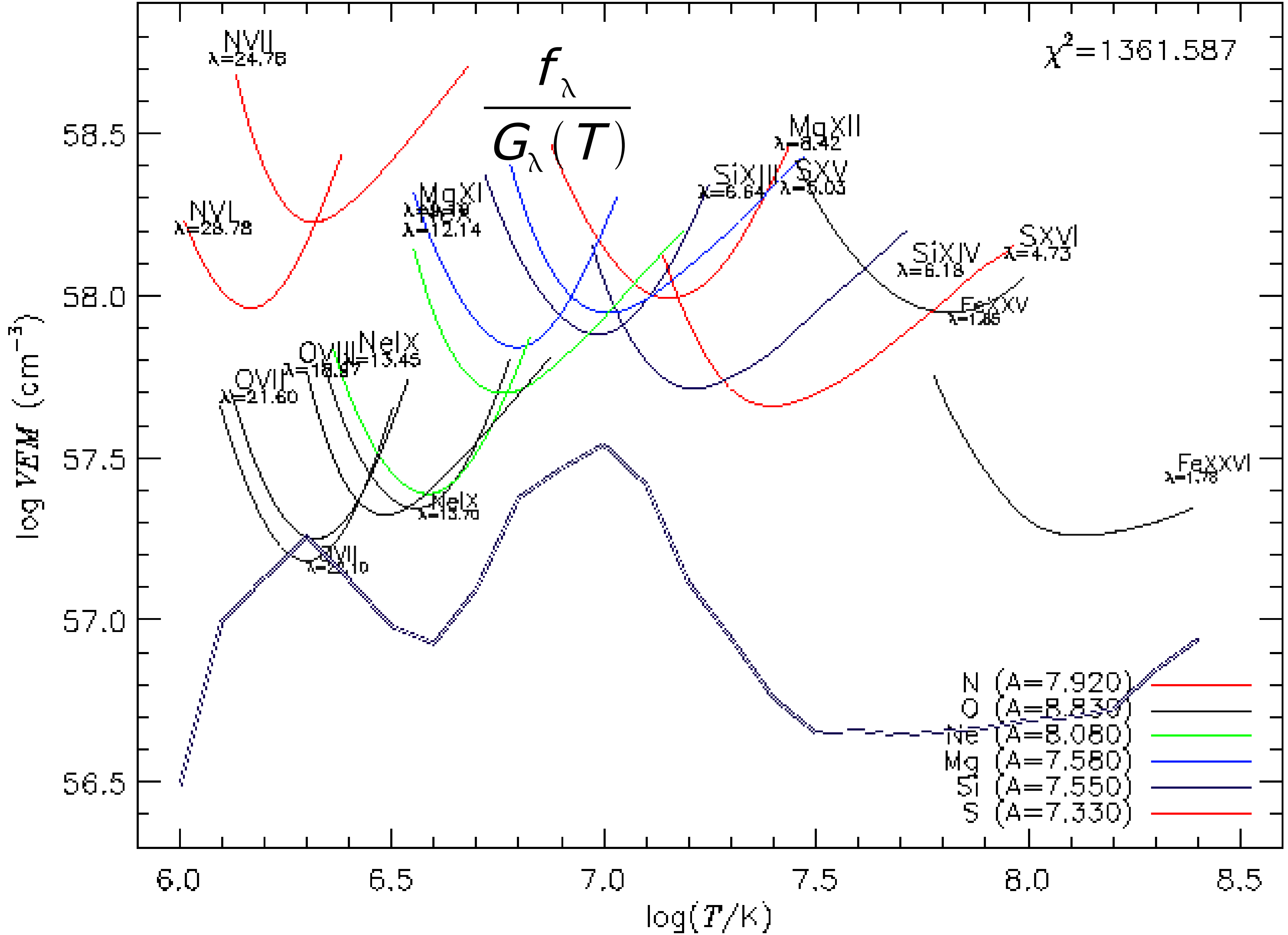

$\frac{f_\lambda}{G_\lambda(T)}$
χ^2=1361.587
NVII λ=24.78
NVI λ=28.78
MgXI
λ=12.14
MgXII λ=8.42
SiXIII λ=6.64
SXV λ=5.03
SiXIV λ=6.18
SXVI λ=4.73
FeXXV λ=1.85
FeXXVI λ=1.78
OVIII λ=18.97
NeIX λ=13.45
OVII λ=21.60
NeIX λ=13.70
OVII
58.5
58.0
57.5
57.0
56.5
6.0
6.5
7.0
7.5
8.0
8.5
log VEM (cm^{-3})
log(T/K)
N (A=7.920)
O (A=8.830)
Ne (A=8.080)
Mg (A=7.580)
Si (A=7.550)
S (A=7.330)

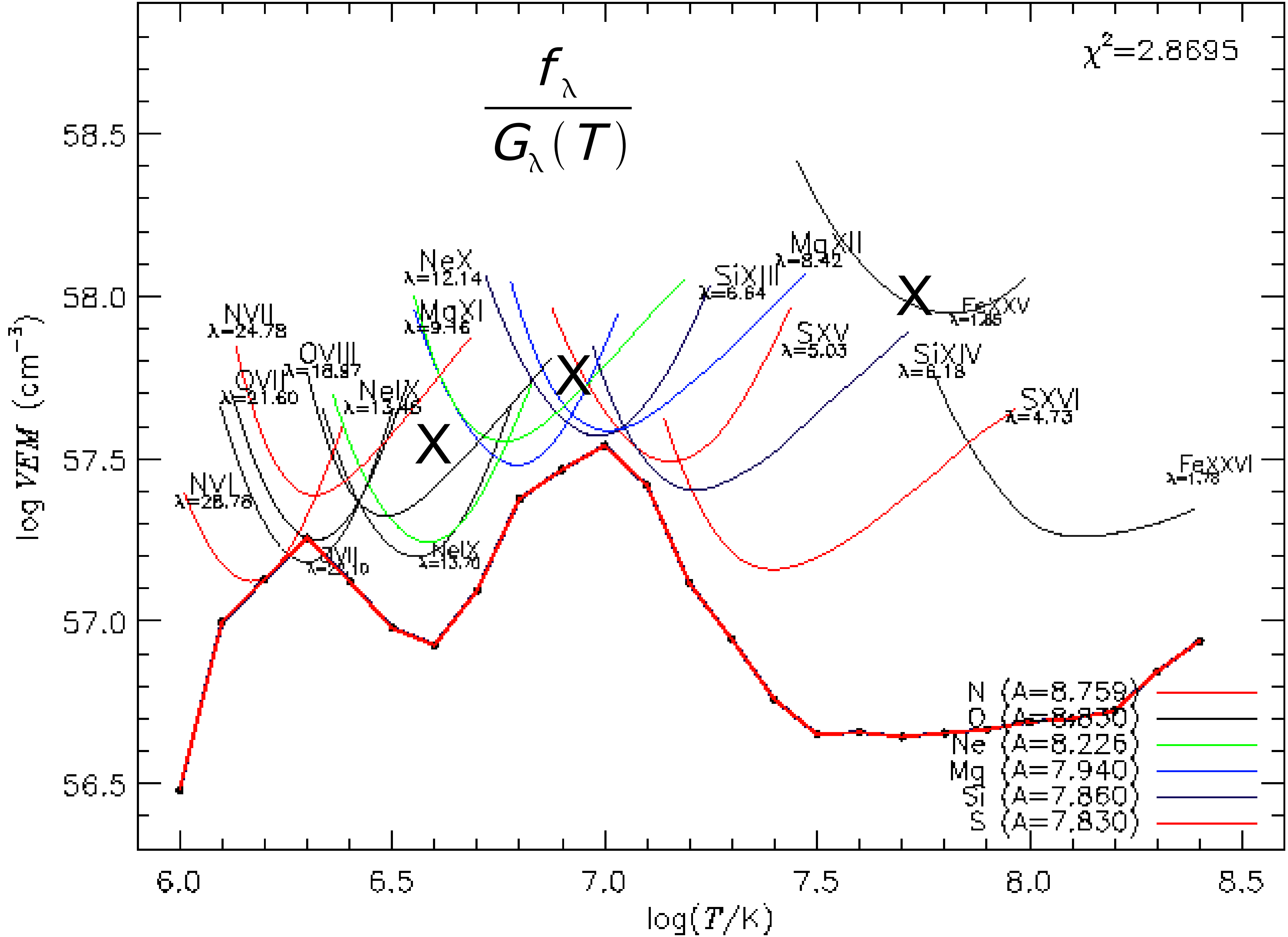

$\frac{f_\lambda}{G_\lambda(T)}$
$\chi^2=2.8695$
log VEM (cm^{-3})
log(T/K)
NeX λ=12.14
MgXI λ=9.16
NVII λ=24.78
OVIII λ=18.97
OVII λ=21.60
NeIX λ=13.45
NVI λ=28.78
OVII λ=22.10
NeIX λ=13.70
SiXIII λ=6.64
MgXII λ=8.42
FeXXV λ=1.85
SXV λ=5.03
SiXIV λ=6.18
SXVI λ=4.73
FeXXVI λ=1.78
N (A=8.759)
O (A=8.830)
Ne (A=8.226)
Mg (A=7.940)
Si (A=7.860)
S (A=7.830)

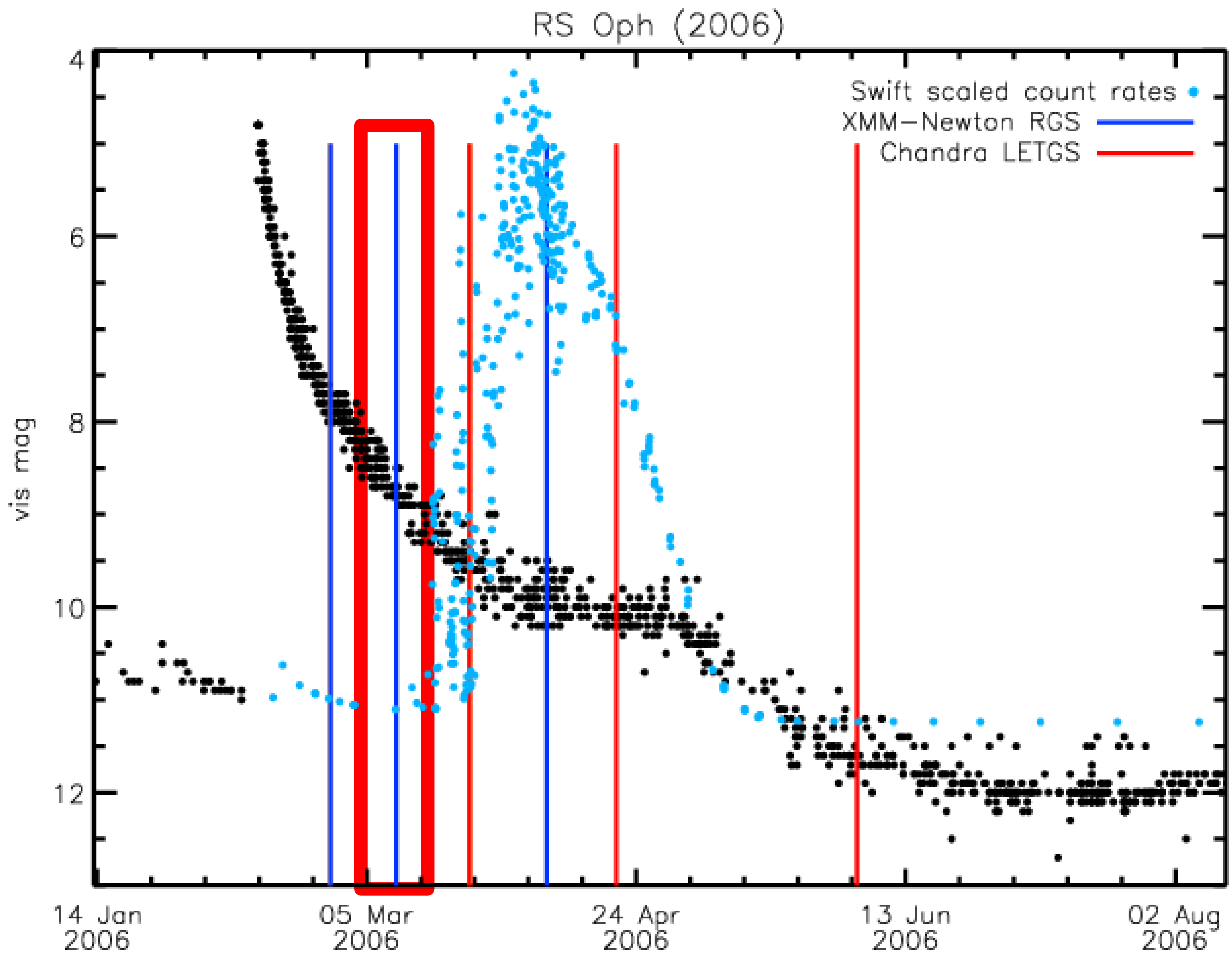

RS Oph (2006)
Swift scaled count rates
XMM-Newton RGS
Chandra LETGS
vis mag
4
6
8
10
12
14 Jan 2006
05 Mar 2006
24 Apr 2006
13 Jun 2006
02 Aug 2006

Recurrent Nova RS Oph, day 26.1

XMM-Newton multi-λ light curve

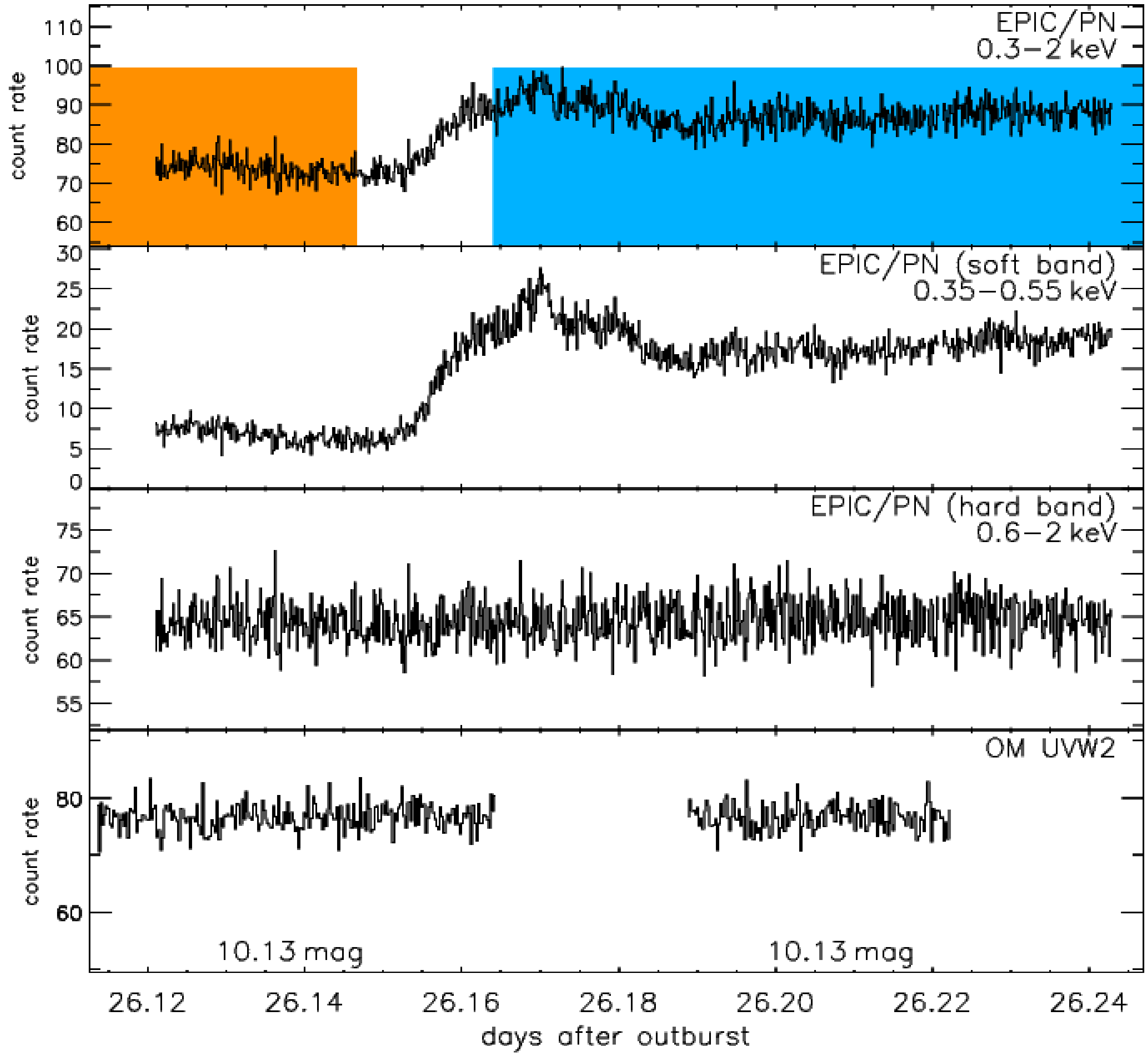

Recurrent Nova RS Oph, day 26.1

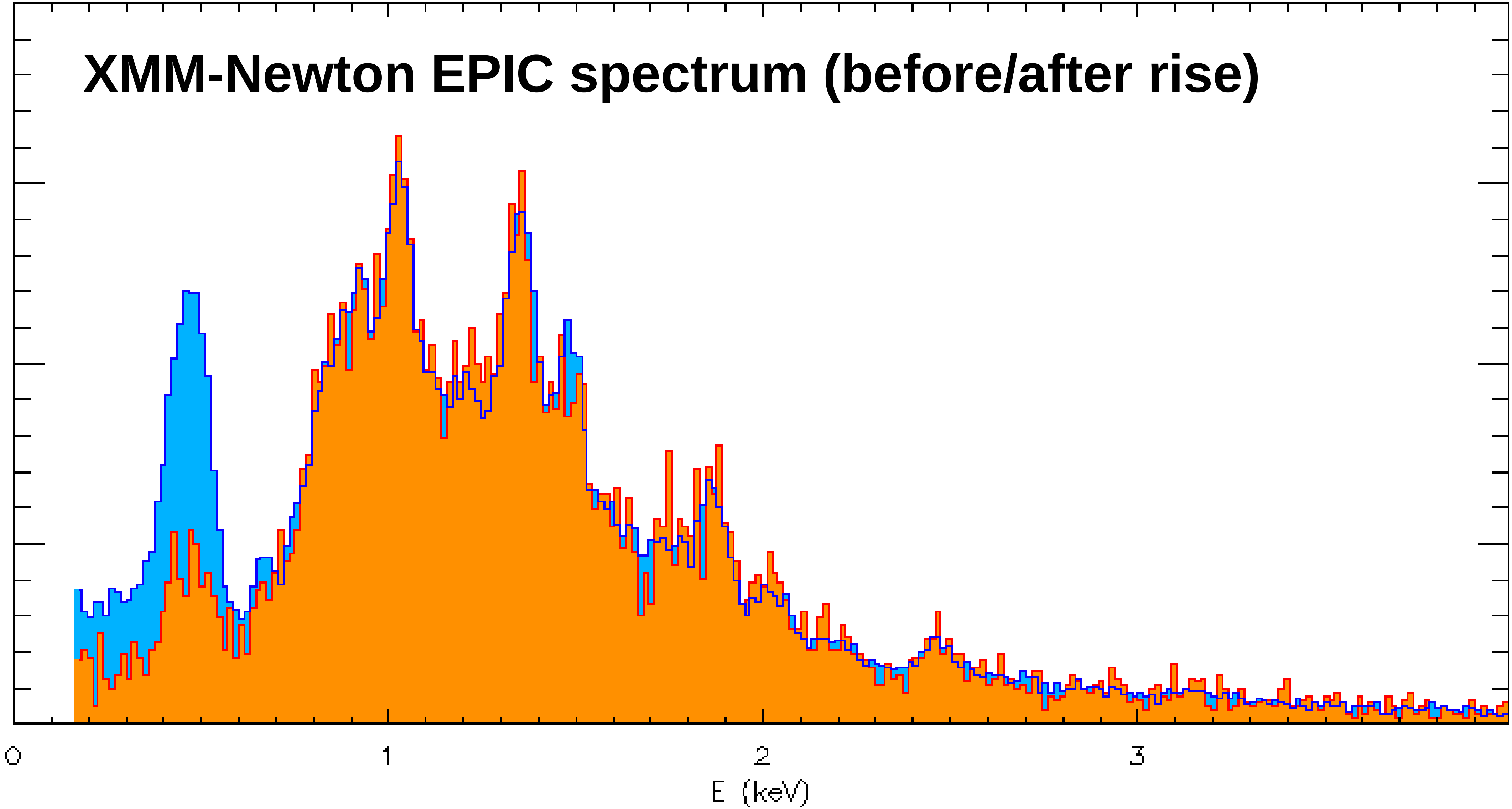

Recurrent Nova RS Oph, day 26.1

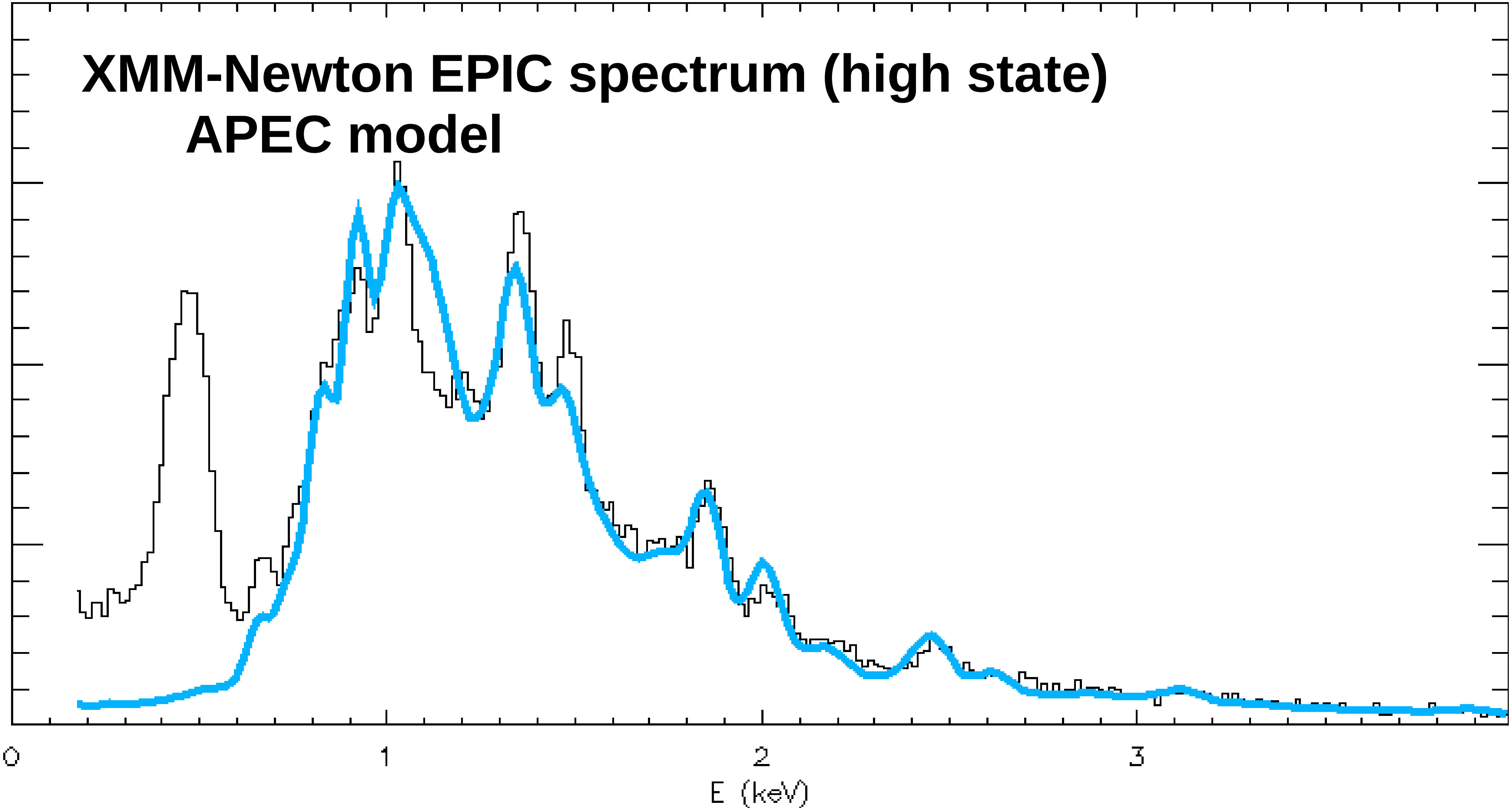

Recurrent Nova RS Oph, day 26.1

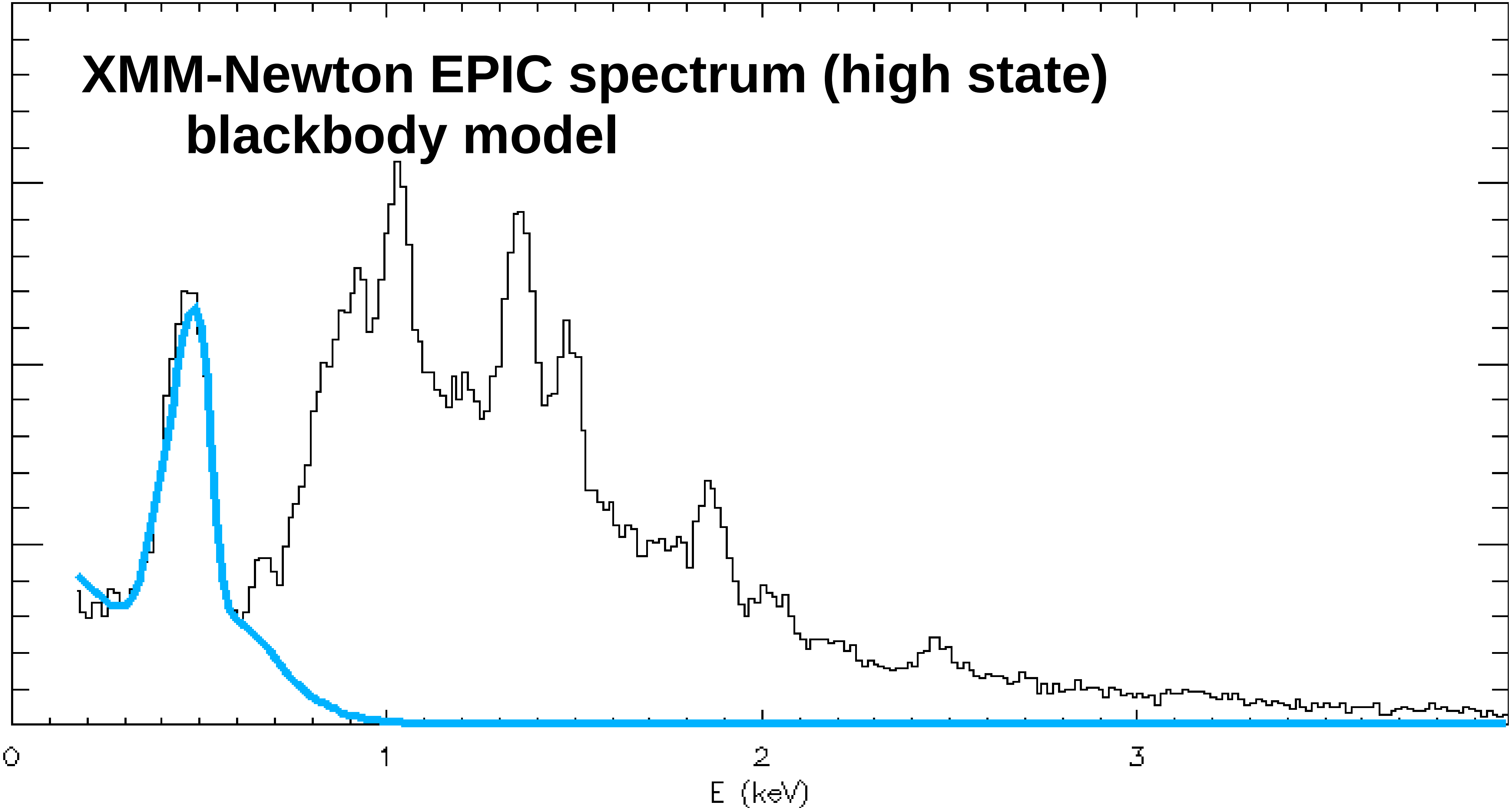

Recurrent Nova RS Oph, day 26.1

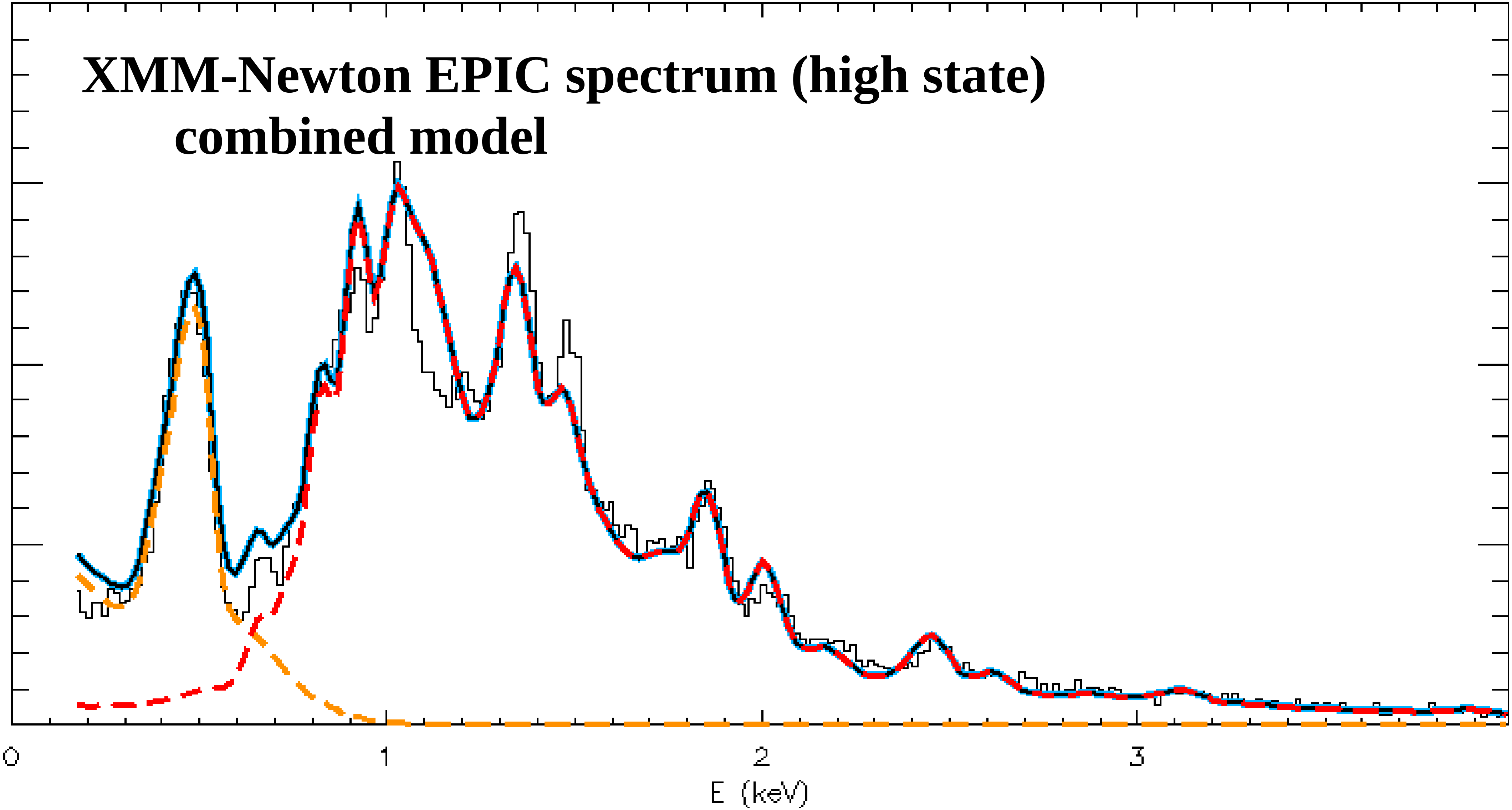

Recurrent Nova RS Oph, day 26.1

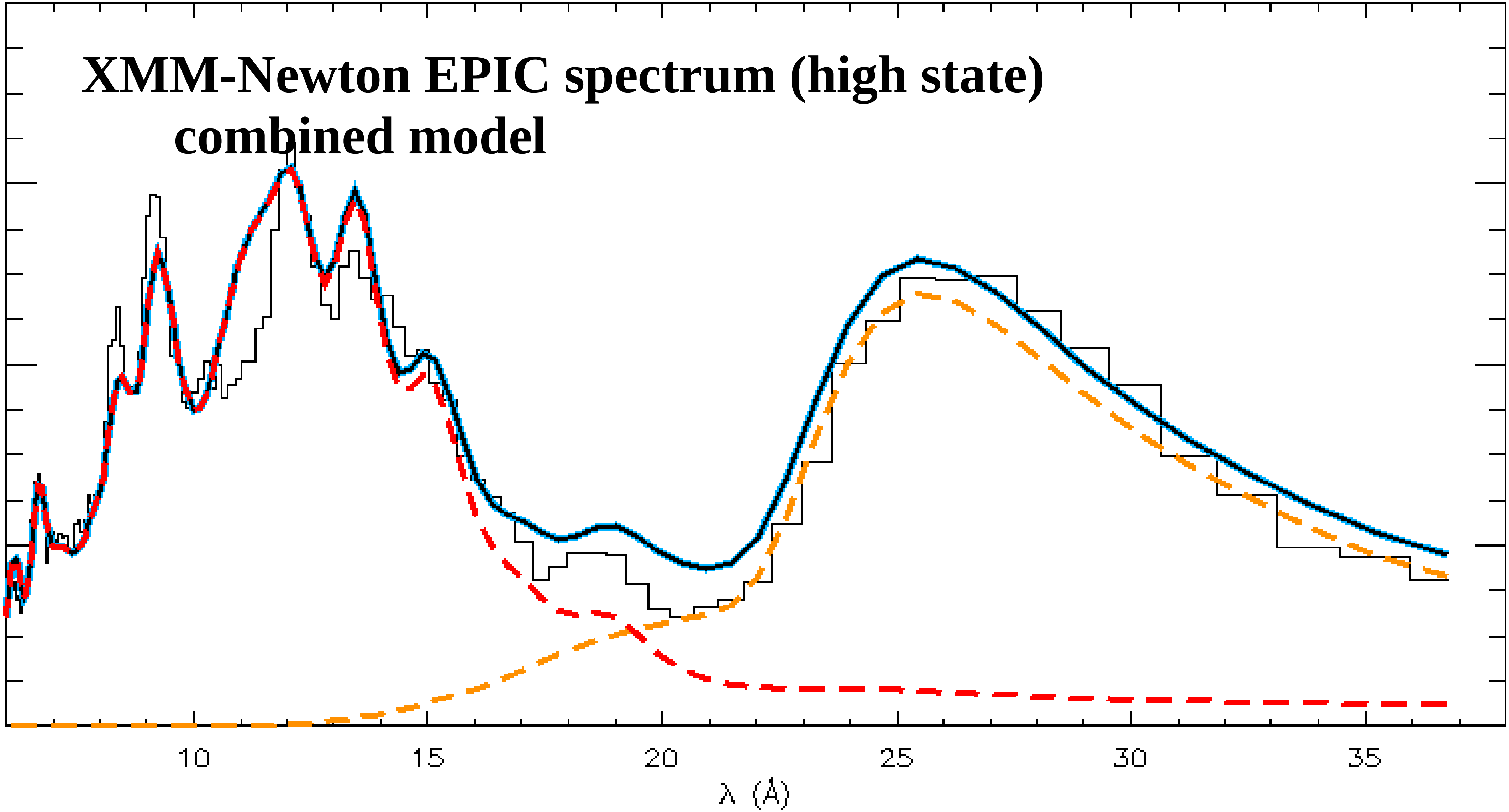

Recurrent Nova RS Oph, day 26.1

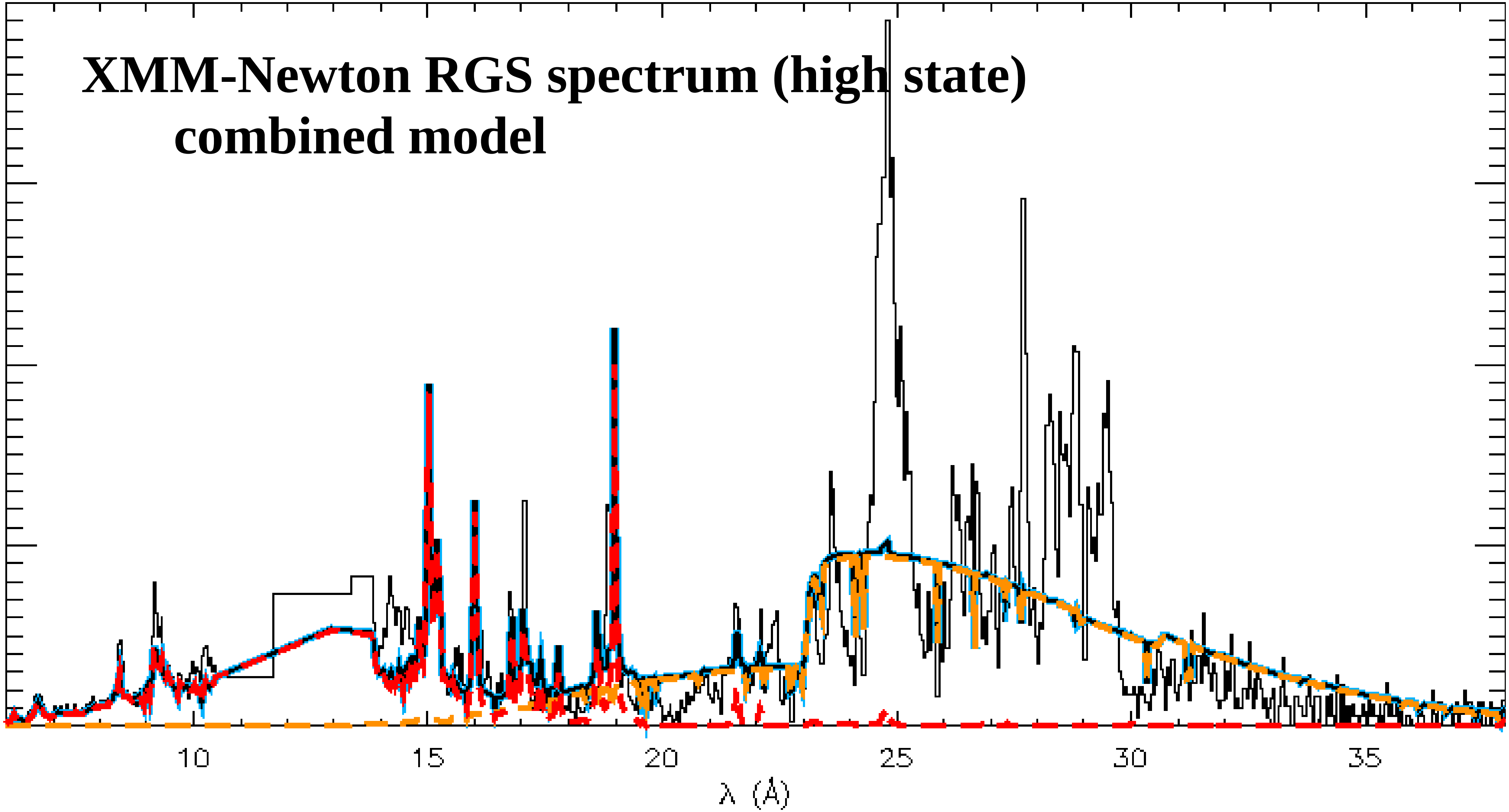

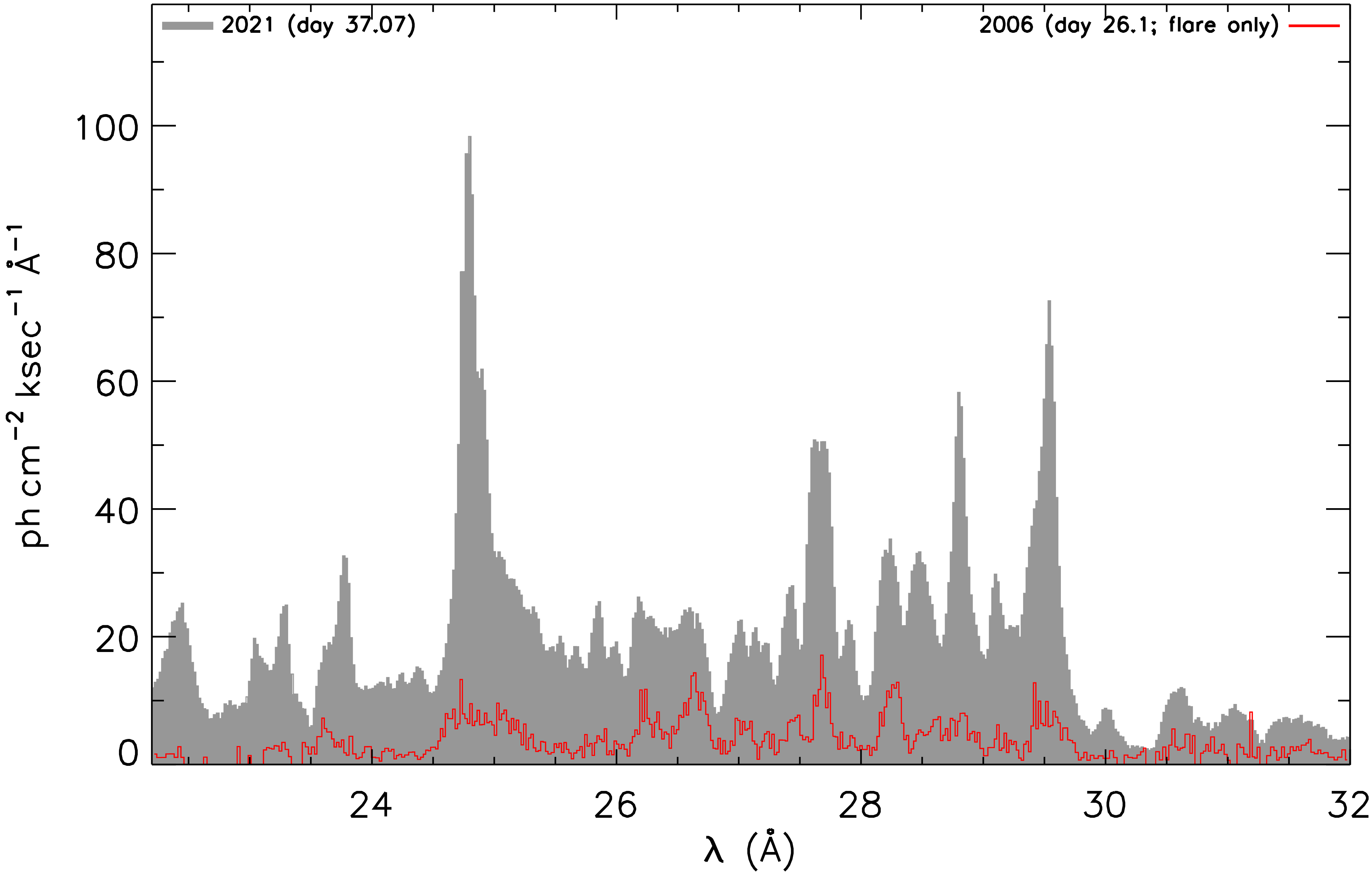

2021 (day 37.07)
2006 (day 26.1; flare only)
ph cm^{-2} ksec^{-1} Å^{-1}
0
20
40
60
80
100
24
26
28
30
32
λ (Å)

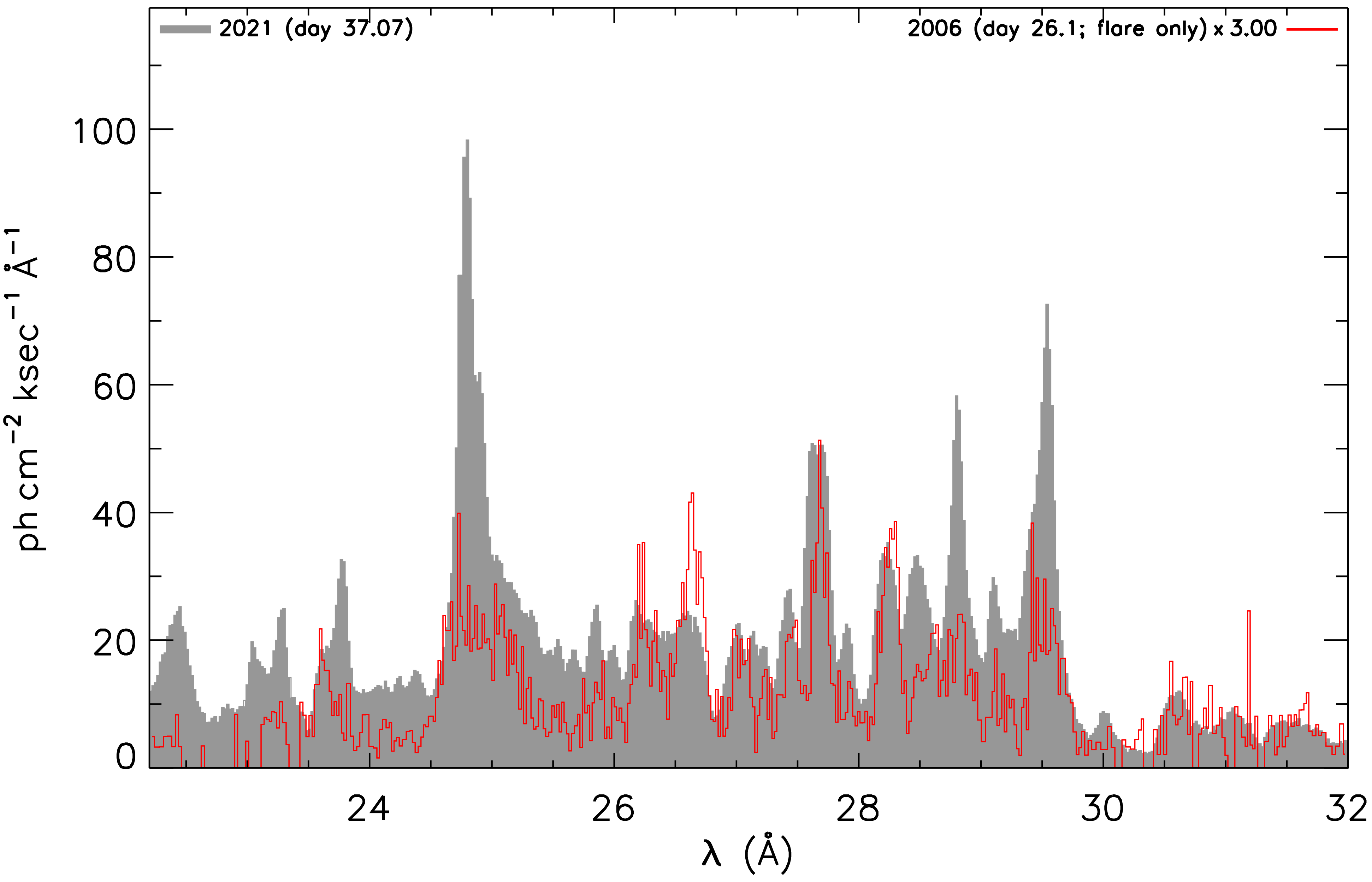

2021 (day 37.07)
2006 (day 26.1; flare only) x 3.00
100
80
60
40
20
0
ph cm^{-2} ksec^{-1} Å^{-1}
24
26
28
30
32
λ (Å)

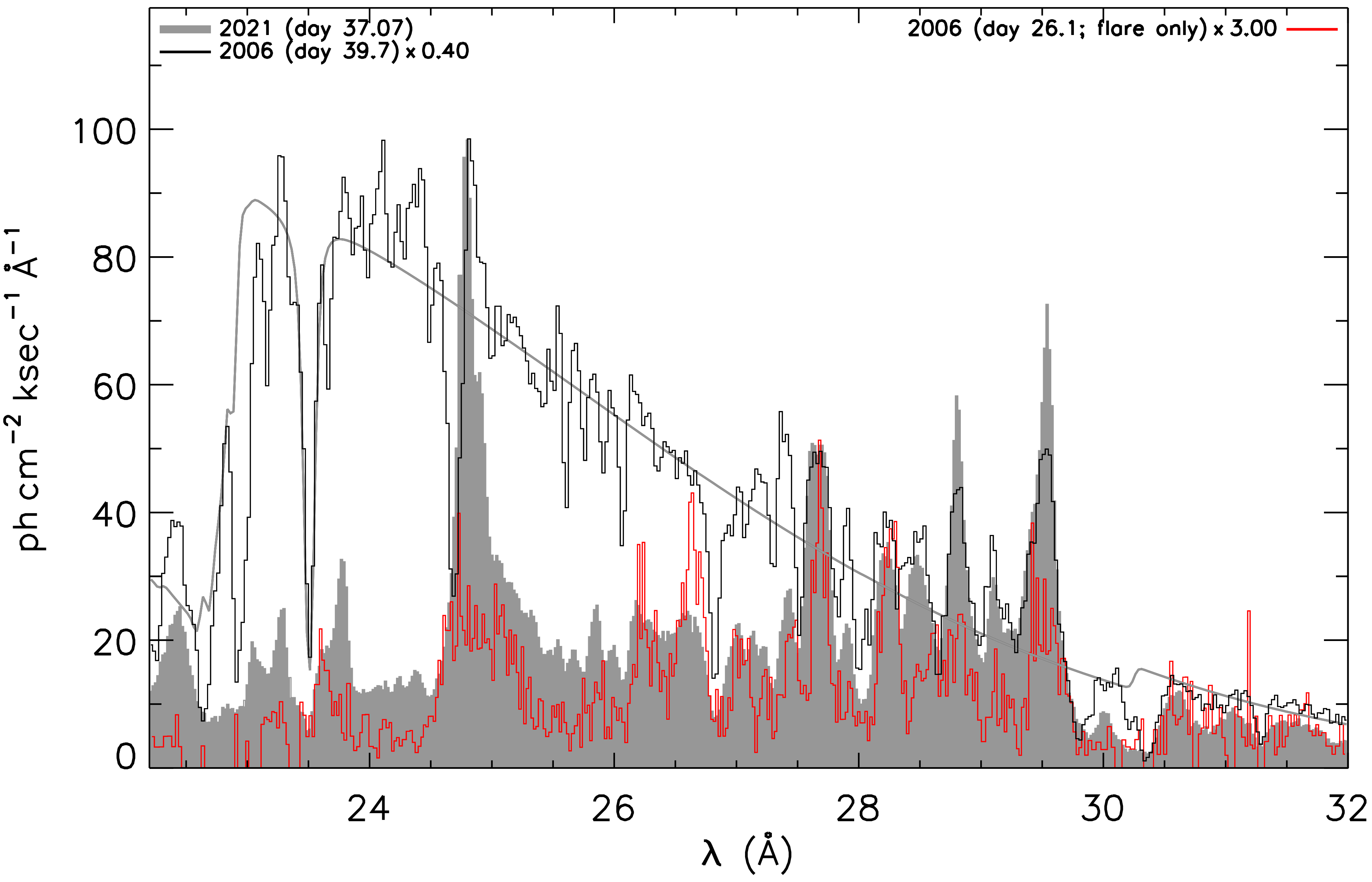

2021 (day 37.07)
2006 (day 39.7) x 0.40
2006 (day 26.1; flare only) x 3.00
ph cm^{-2} ksec^{-1} Å^{-1}
0
20
40
60
80
100
24
26
28
30
32
λ (Å)

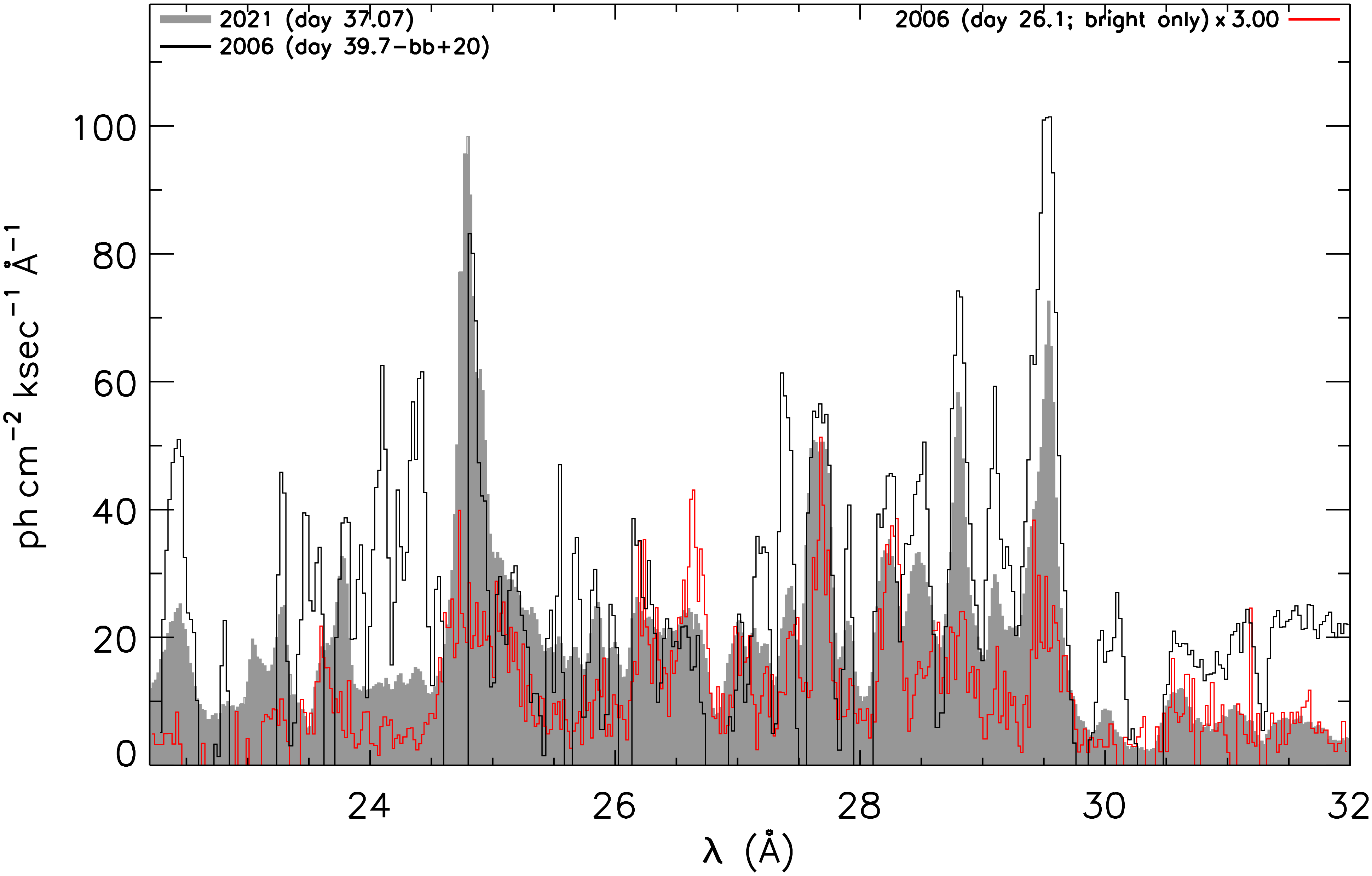
2021 (day 37.07)
2006 (day 39.7−bb+20)
2006 (day 26.1; bright only) x 3.00
ph cm^{-2} ksec^{-1} Å^{-1}
λ (Å)
0
20
40
60
80
100
24
26
28
30
32

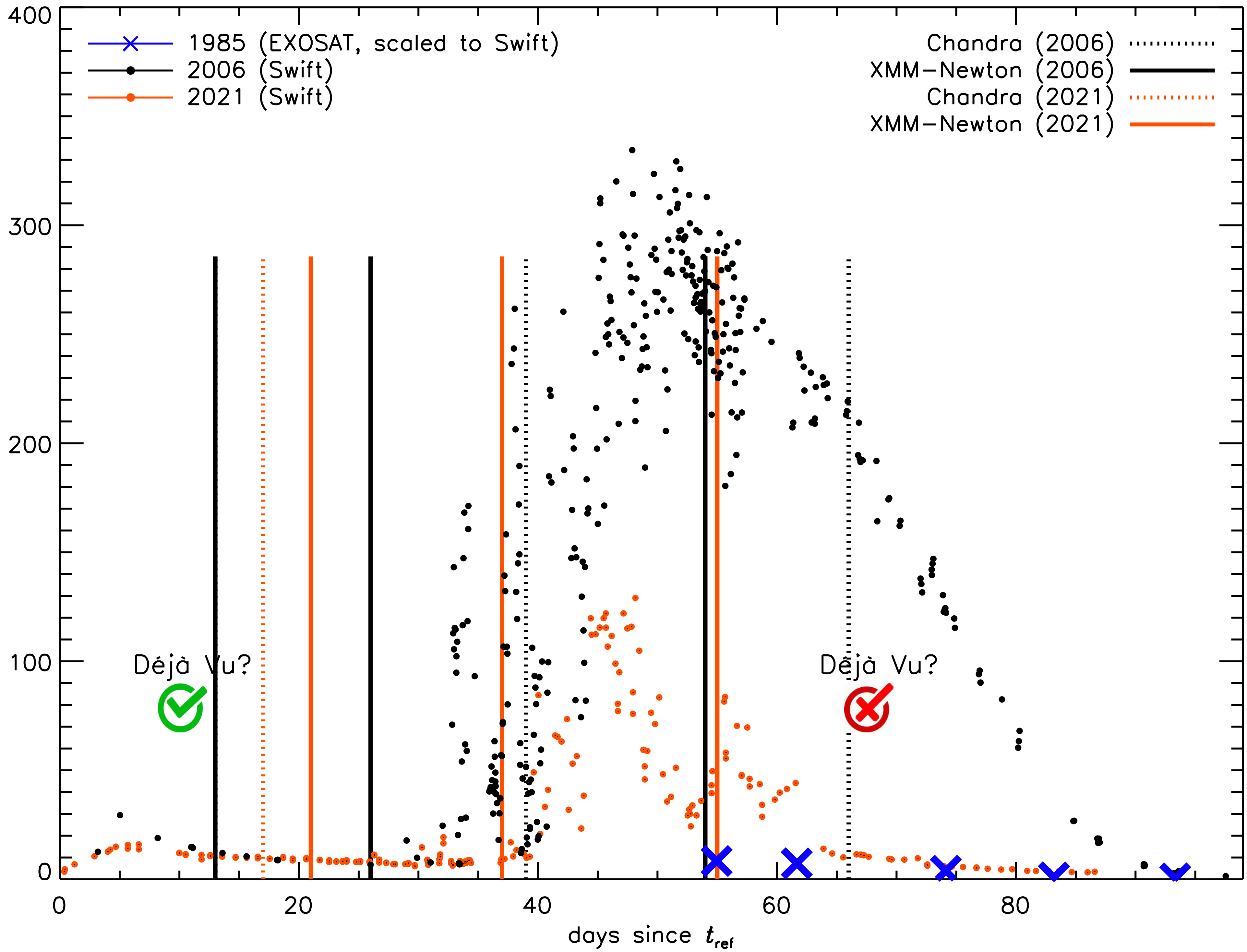

400
300
200
100
0
0
20
40
60
80
days since t_{ref}
1985 (EXOSAT, scaled to Swift)
2006 (Swift)
2021 (Swift)
Chandra (2006)
XMM–Newton (2006)
Chandra (2021)
XMM–Newton (2021)
Déjà Vu?
Déjà Vu?

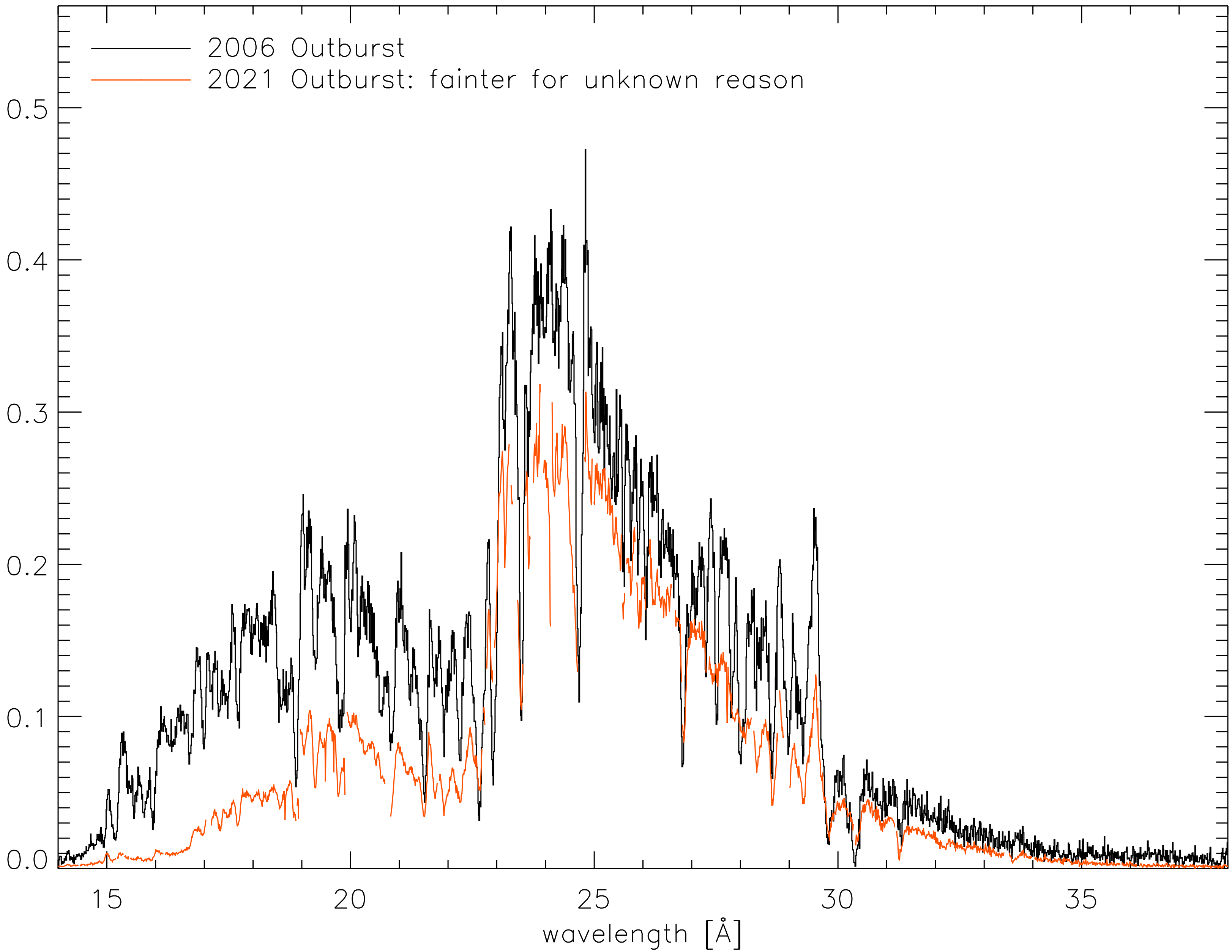

2006 Outburst
2021 Outburst: fainter for unknown reason
0.0
0.1
0.2
0.3
0.4
0.5
15
20
25
30
35
wavelength [Å]

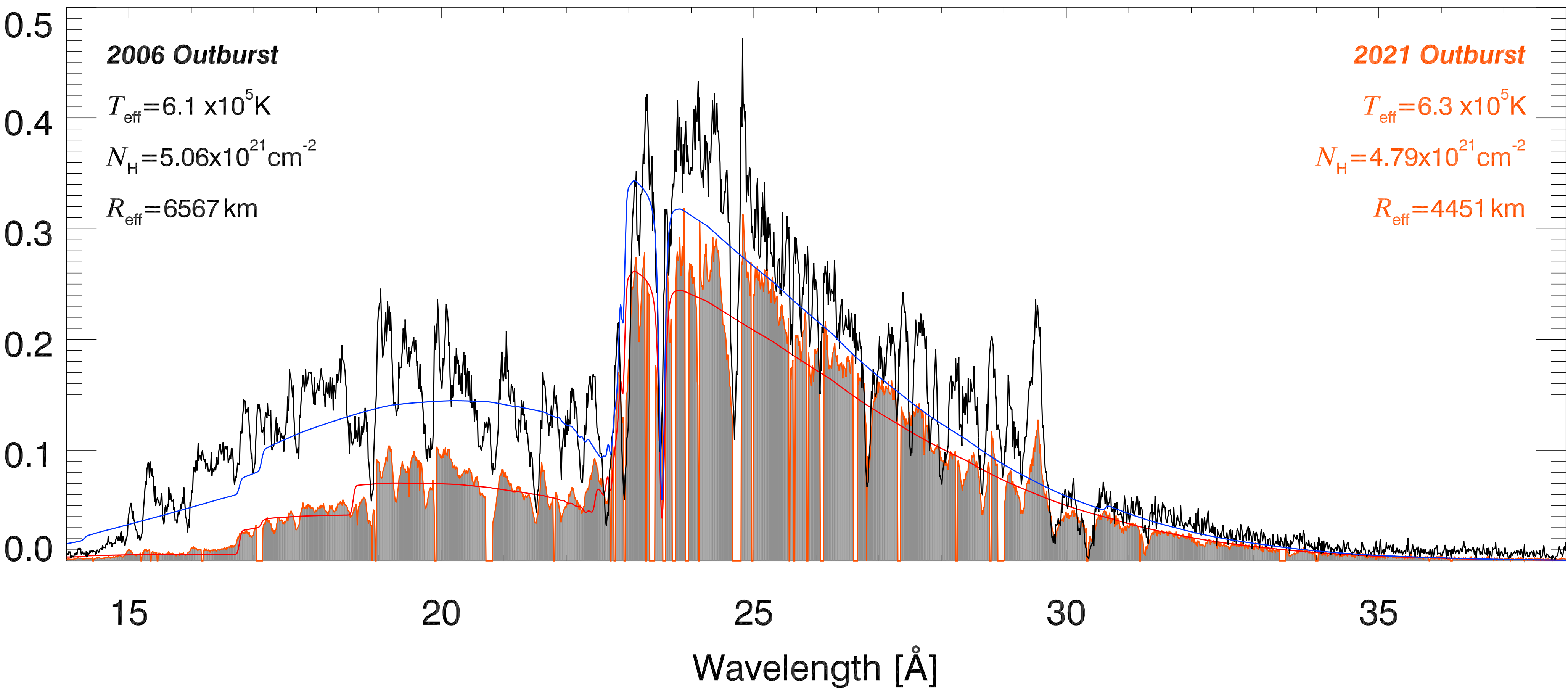

2006 Outburst
T_{eff}=6.1 x10^{5}K
N_{H}=5.06x10^{21}cm^{-2}
R_{eff}=6567 km
2021 Outburst
T_{eff}=6.3 x10^{5}K
N_{H}=4.79x10^{21}cm^{-2}
R_{eff}=4451 km
0.0
0.1
0.2
0.3
0.4
0.5
15
20
25
30
35
Wavelength [Å]

Series of SSS spectra of V4743 Sgr with TMAP Atmospheres Rauch et al. (2010)

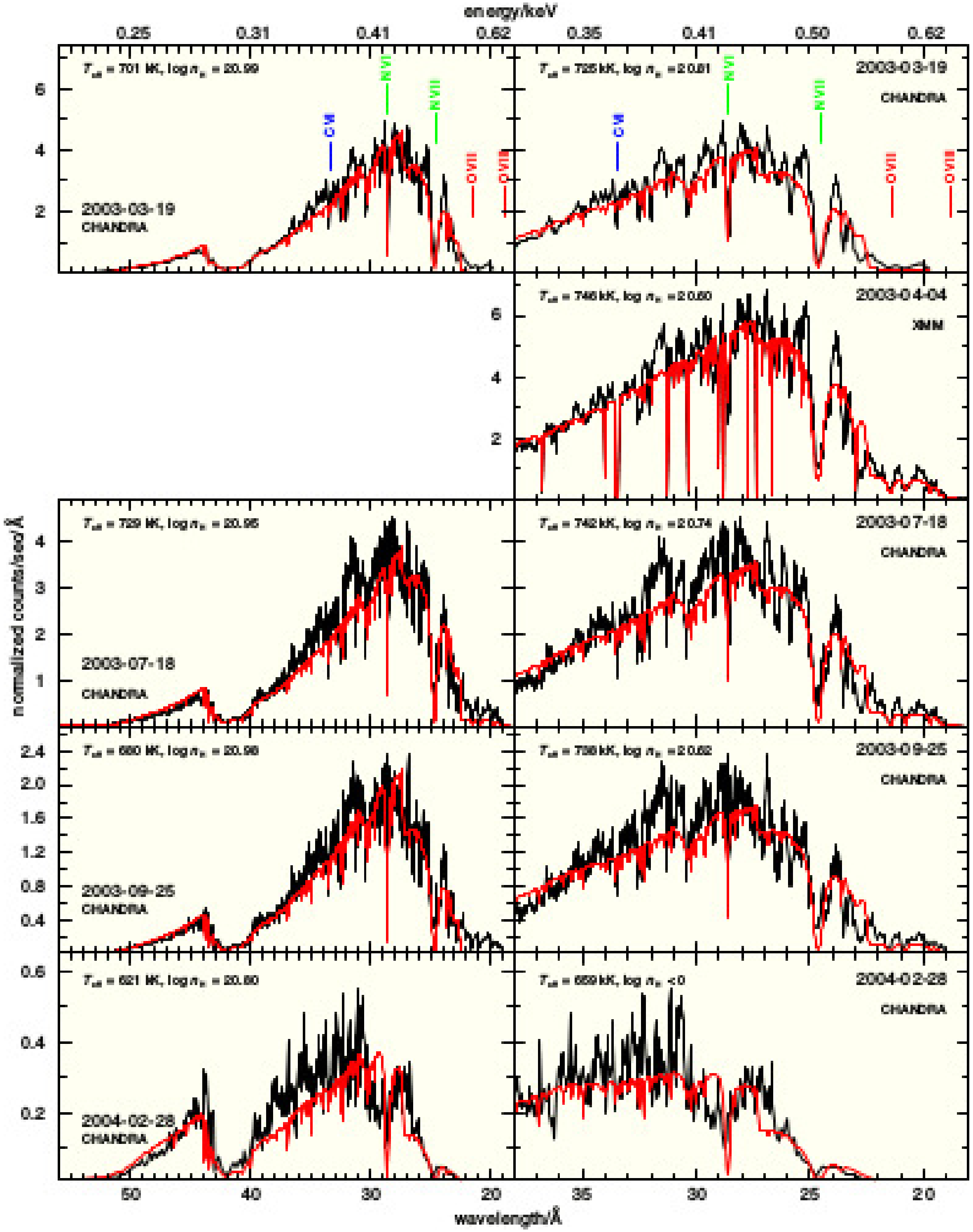

Series of SSS spectra of V4743 Sgr with Wind-type Atmospheres van Rossum (2012)

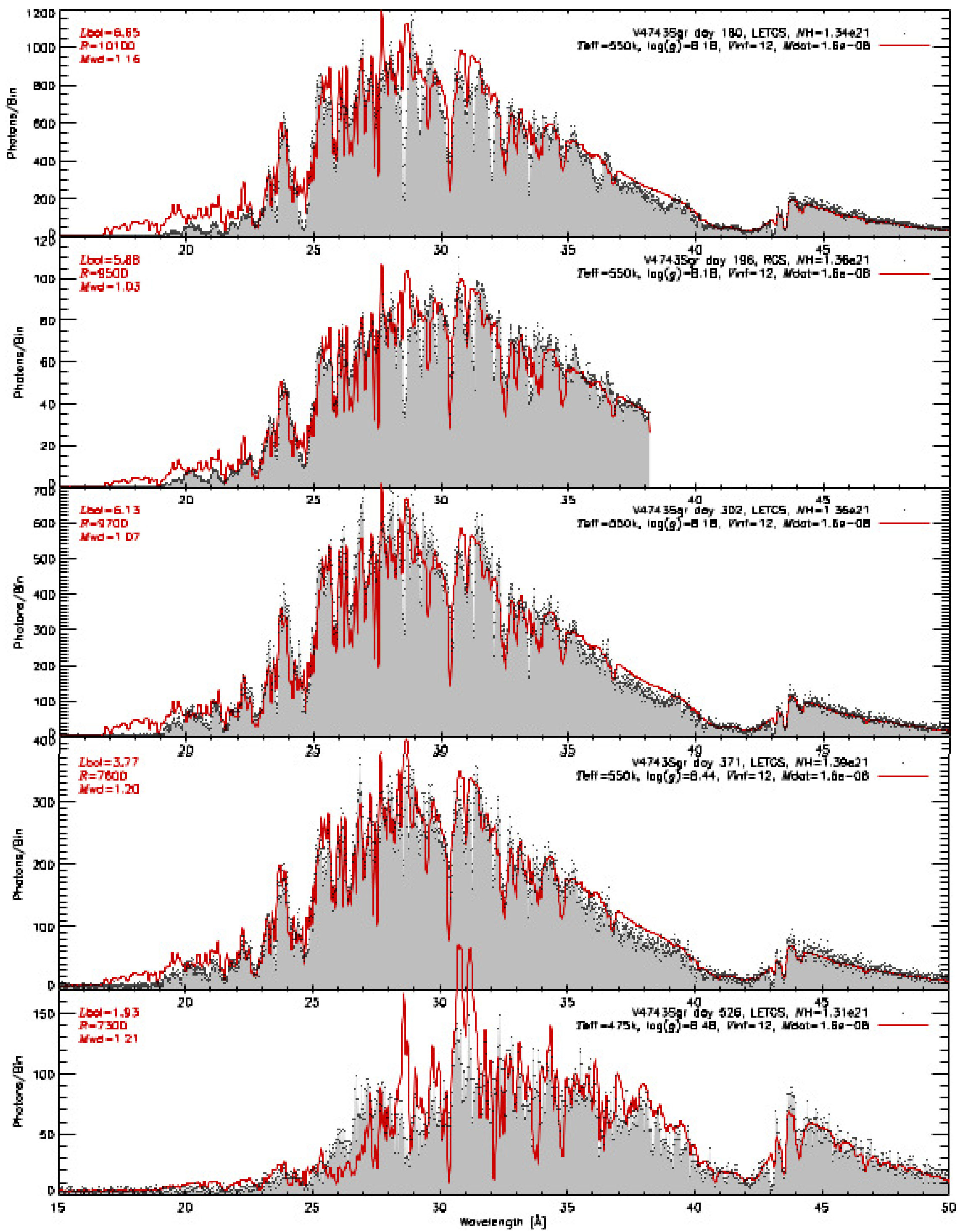

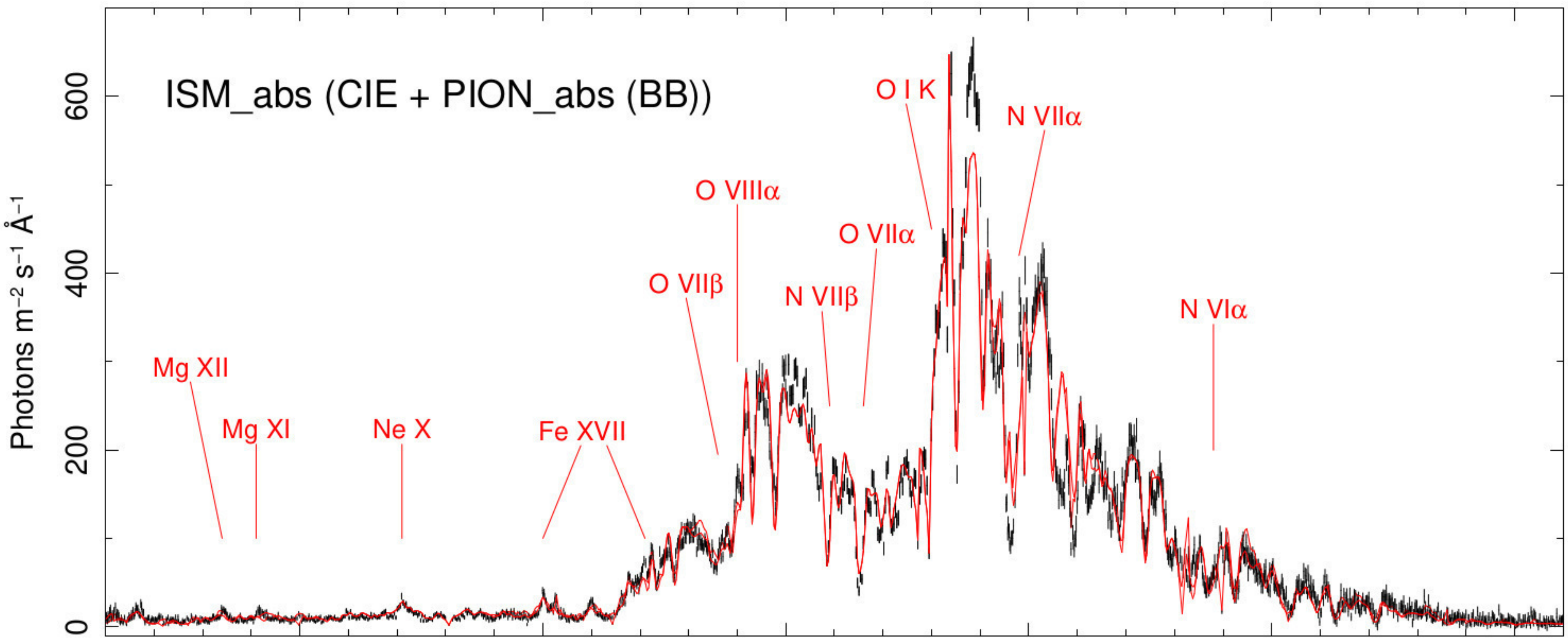
ISM_abs (CIE + PION_abs (BB))
Photons m^{-2} s^{-1} Å^{-1}
0
200
400
600
Mg XII
Mg XI
Ne X
Fe XVII
O VIIβ
O VIIIα
N VIIβ
O VIIα
O I K
N VIIα
N VIα

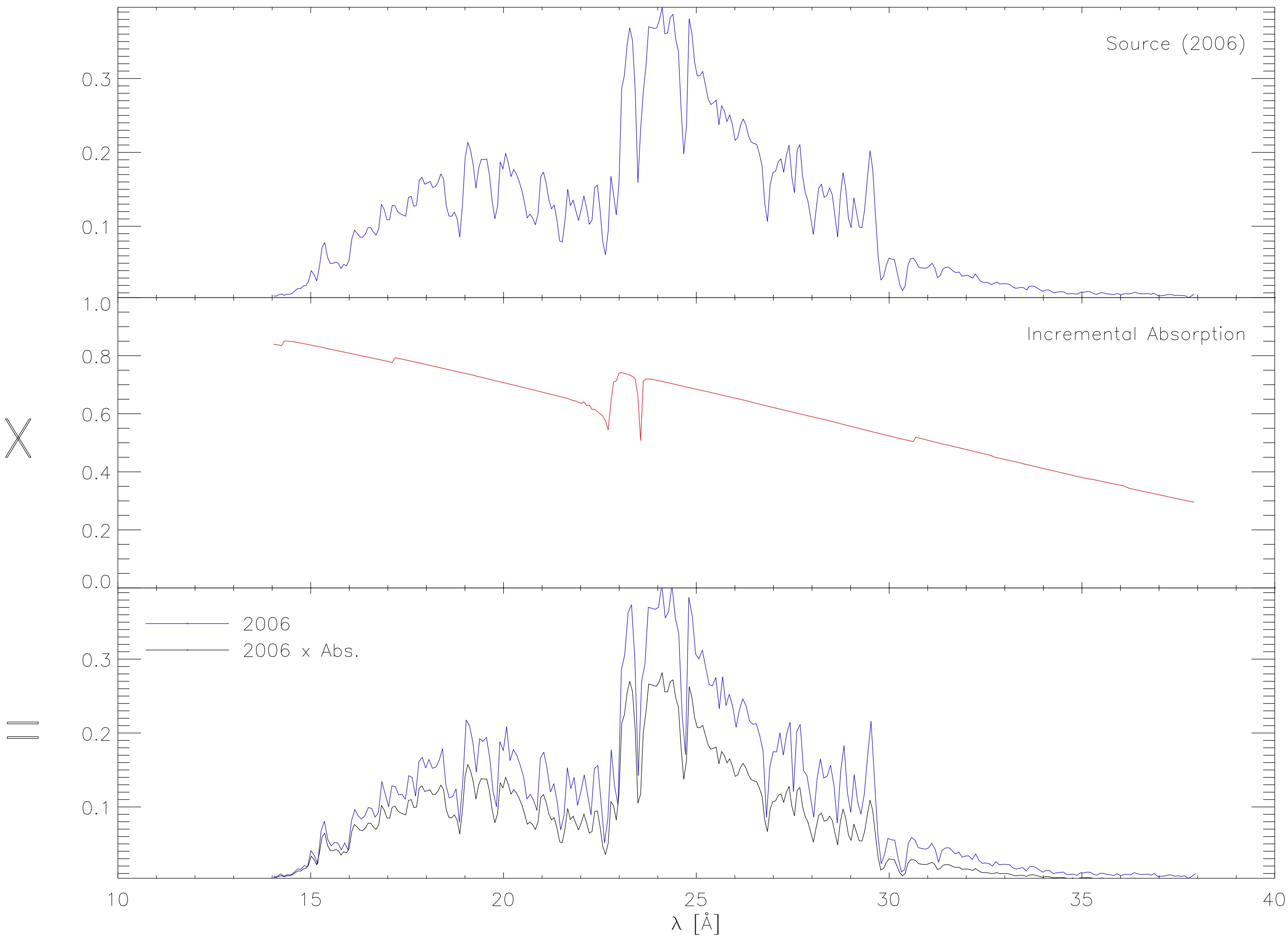
Source (2006)
Incremental Absorption
X
=
2006
2006 x Abs.
0.1
0.2
0.3
0.0
0.2
0.4
0.6
0.8
1.0
10
15
20
25
30
35
40
λ [Å]

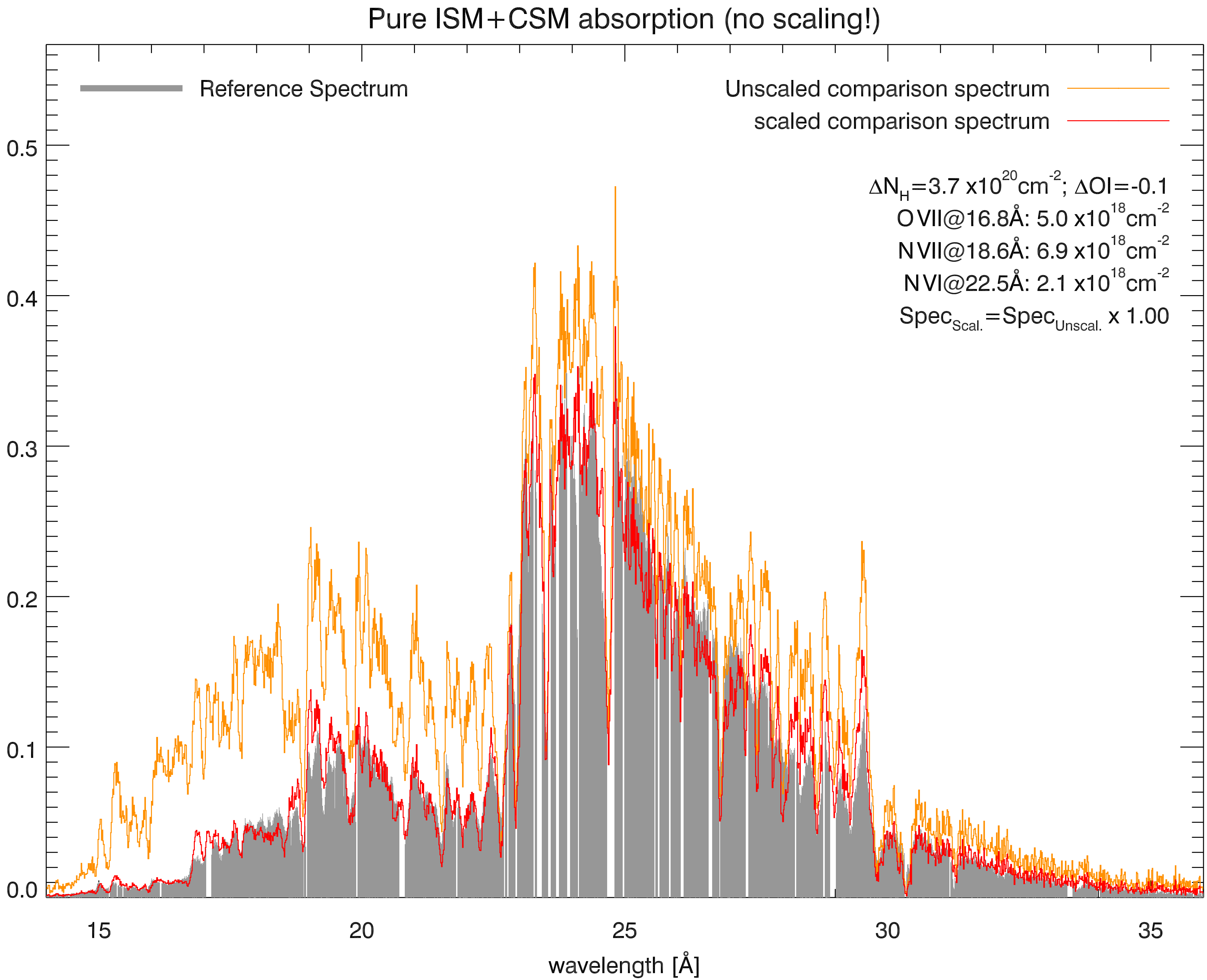
Pure ISM+CSM absorption (no scaling!)
Reference Spectrum
Unscaled comparison spectrum
scaled comparison spectrum
ΔN_H=3.7 x10^20 cm^-2; ΔOI=-0.1
O VII@16.8Å: 5.0 x10^18 cm^-2
N VII@18.6Å: 6.9 x10^18 cm^-2
N VI@22.5Å: 2.1 x10^18 cm^-2
Spec_Scal.=Spec_Unscal. x 1.00
0.0
0.1
0.2
0.3
0.4
0.5
15
20
25
30
35
wavelength [Å]

Typical X-ray Grating Spectra of SSS

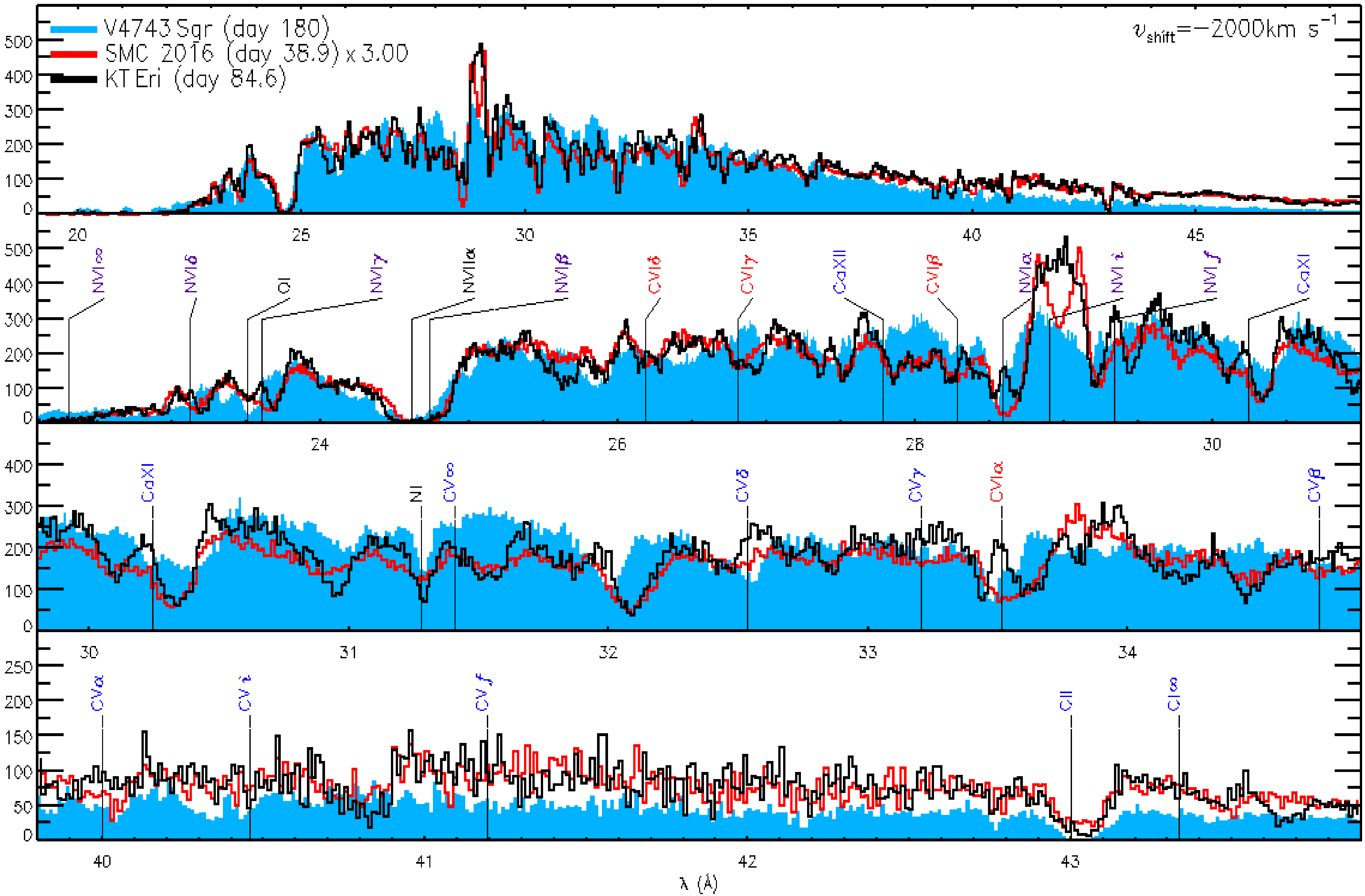

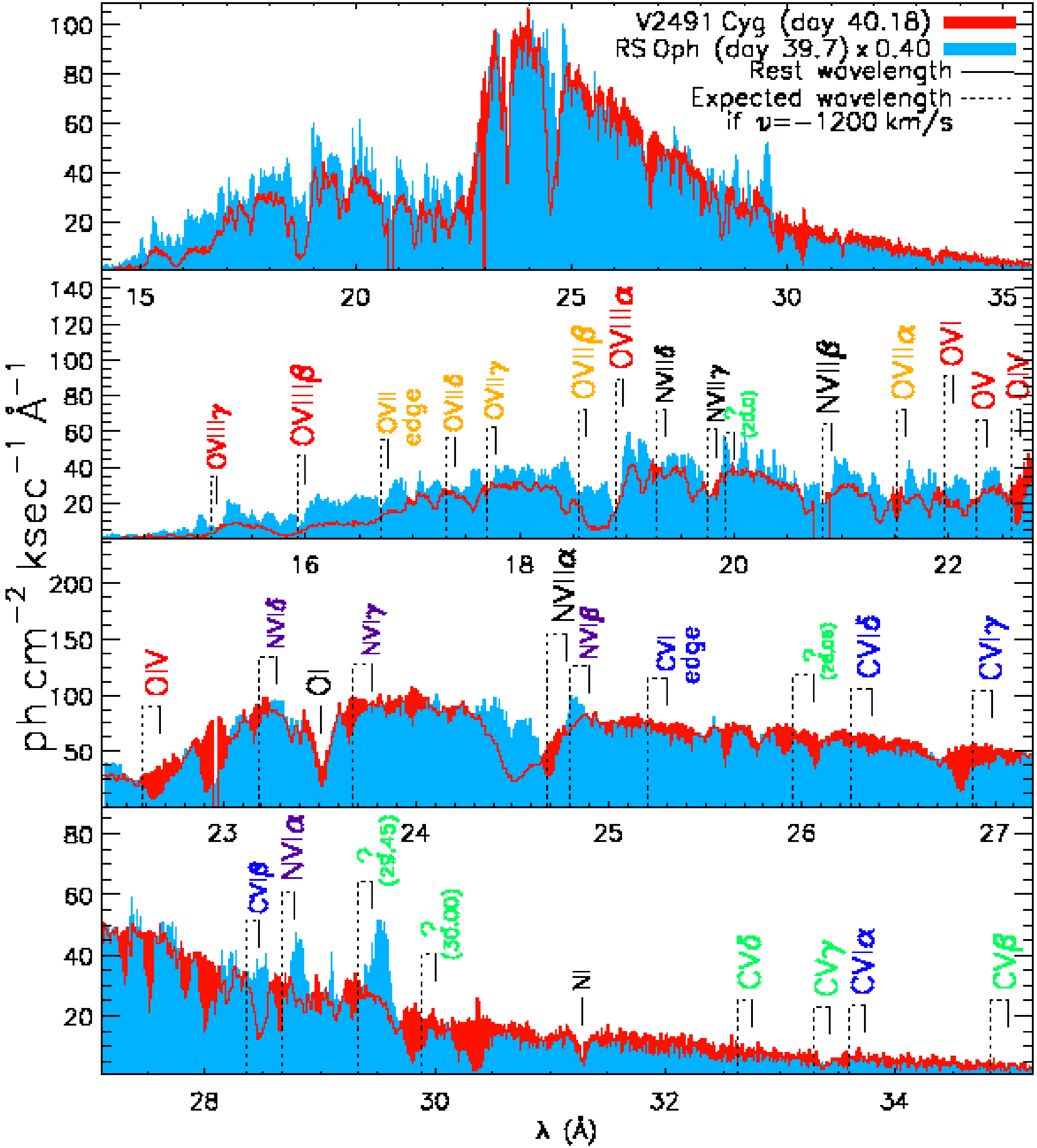

V2491 Cyg (day 40.18)
RS Oph (day 39.7) x 0.40
Rest wavelength
Expected wavelength
if v=−1200 km/s
ph cm^{-2} ksec^{-1} Å^{-1}
λ (Å)
OVIIIγ
OVIIIβ
OVII edge
OVIIδ
OVIIγ
OVIIβ
OVIIIα
NVIIδ
NVIIγ
? (zd,a)
NVIIβ
OVIIα
OVI
OV
OIV
OI
NVIδ
NVIγ
NVIIα
NVIβ
CVI edge
? (zd,as)
CVIδ
CVIγ
CVIβ
NVIα
? (zd,45)
? (30,00)
NI
CVδ
CVγ
CVIα
CVβ

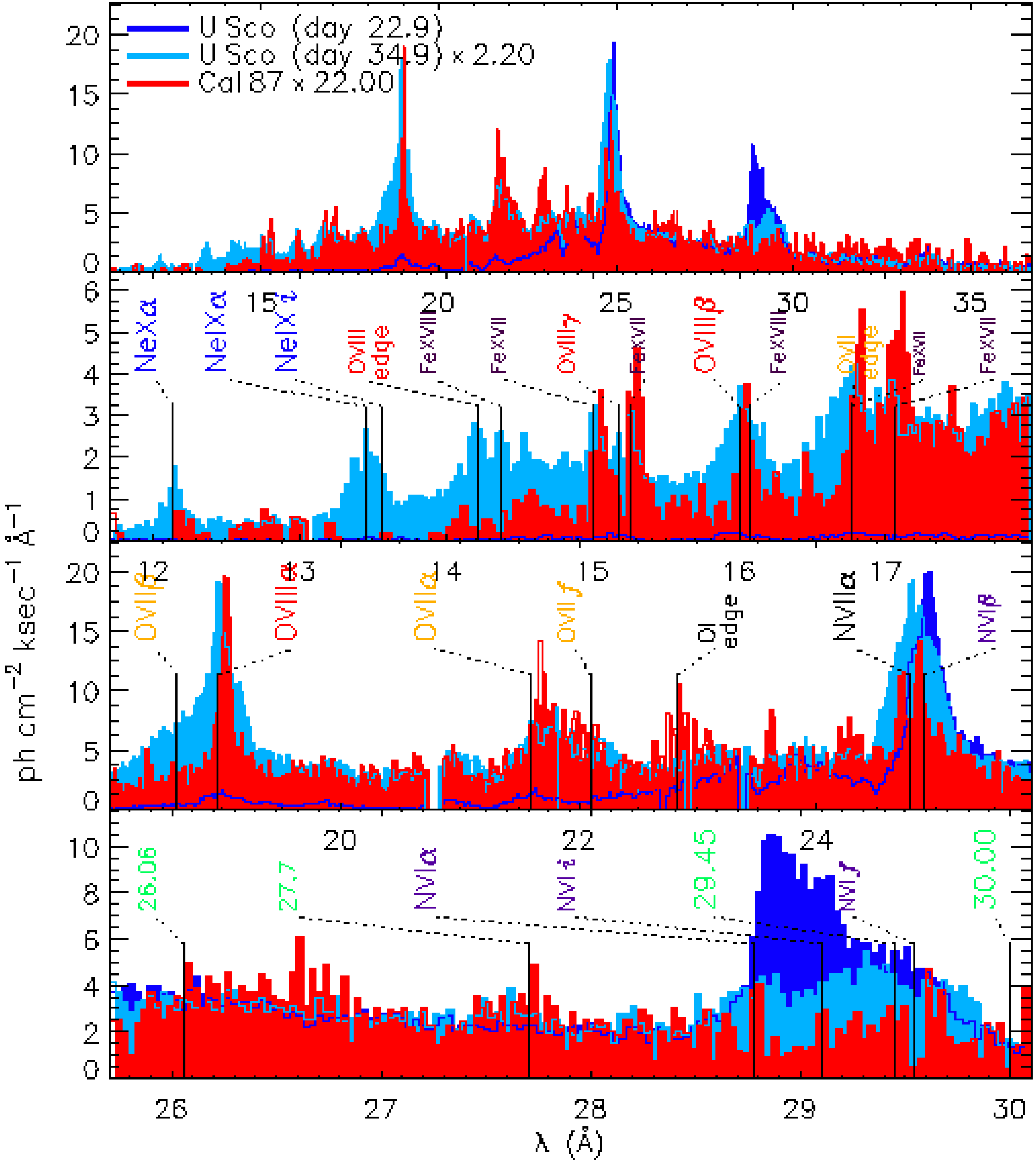

U Sco (day 22.9)
U Sco (day 34.9) × 2.20
Cal 87 × 22.00
NeXα
NeIXα
NeIXi
OVIII edge
FeXVIII
FeXVII
OVIIIγ
OVIIIβ
OVII edge
OVIIβ
OVIIIα
OVIIα
OVII f
OI edge
NVIIα
NVIβ
26.06
27.7
NVIα
NVI i
29.45
NVI f
30.00
ph cm^{-2} ksec^{-1} Å^{-1}
λ (Å)

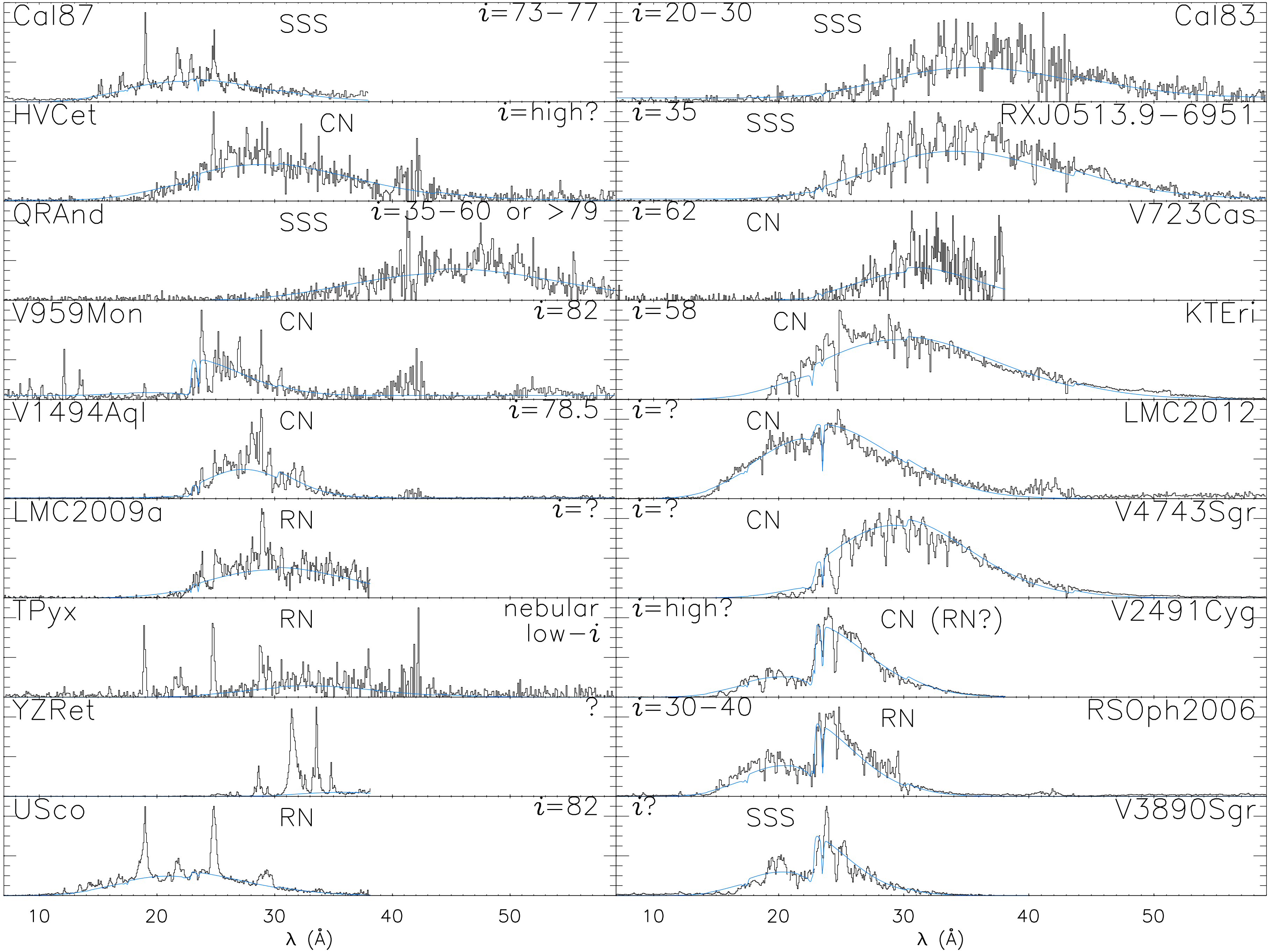

Cal87
SSS
i=73−77
i=20−30
SSS
Cal83
HVCet
CN
i=high?
i=35
SSS
RXJ0513.9−6951
QRAnd
SSS
i=35−60 or >79
i=62
CN
V723Cas
V959Mon
CN
i=82
i=58
CN
KTEri
V1494Aql
CN
i=78.5
i=?
CN
LMC2012
LMC2009a
RN
i=?
i=?
CN
V4743Sgr
TPyx
RN
nebular
low−i
i=high?
CN (RN?)
V2491Cyg
YZRet
?
i=30−40
RN
RSOph2006
USco
RN
i=82
i?
SSS
V3890Sgr
10
20
30
40
50
λ (Å)
10
20
30
40
50
λ (Å)